Biophysical Chemistry 300 (2023) 107060

Contents lists available at ScienceDirect

Biophysical Chemistry

journal homepage: www.elsevier.com/locate/biophyschem

Effects of antimicrobial peptides on membrane dynamics: A comparison of fluorescence and NMR experiments

Daniela Roversi [a,1], Cassandra Troiano [a], Evgeniy Salnikov [b], Lorenzo Giordano [a,2], Francesco Riccitelli [a], Marta De Zotti [c], Bruno Casciaro [d], Maria Rosa Loffredo [d], Yoonkyung Park [e], Fernando Formaggio [c], Maria Luisa Mangoni [d], Burkhard Bechinger [b,f], Lorenzo Stella [a,*]

[a] Department of Chemical Science and Technology, University of Rome Tor Vergata, Rome 00133, Italy
[b] RMN et Biophysique des membranes, Institut de Chimie de Strasbourg, CNRS/UMR 7177, Université de Strasbourg, 4, rue Blaise Pascal, Strasbourg 67000, France
[c] Department of Chemical Sciences, University of Padova, Padova 35131, Italy
[d] Department of Biochemical Sciences, Laboratory affiliated to Istituto Pasteur Italia-Fondazione Cenci Bolognetti, Sapienza University of Rome, Rome 00185, Italy.
[e] Department of Biomedical Science and Research Center for Proteinaceous Materials (RCPM), Chosun University, Gwangju, Republic of Korea
[f] Institut Universitaire de France, Paris 75005, France

ARTICLE INFO

Keywords:
Antimicrobial petpides
Membrane dynamics
Fluorescence spectroscopy
NMR spectroscopy

ABSTRACT

Antimicrobial peptides (AMPs) represent a promising class of compounds to fight resistant infections. They are commonly thought to kill bacteria by perturbing the permeability of their cell membranes. However, bacterial killing requires a high coverage of the cell surface by bound peptides, at least in the case of cationic and amphipathic AMPs. Therefore, it is conceivable that peptide accumulation on the bacterial membranes might interfere with vital cellular functions also by perturbing bilayer dynamics, a hypothesis that has been termed "sand in the gearbox". Here we performed a systematic study of such possible effects, for two representative peptides (the cationic cathelicidin PMAP-23 and the peptaibol alamethicin), employing fluorescence and NMR spectroscopies. These approaches are commonly applied to characterize lipid order and dynamics, but sample different time-scales and could thus report on different membrane properties. In our case, fluorescence anisotropy measurements on liposomes labelled with probes localized at different depths in the bilayer showed that both peptides perturb membrane fluidity and order. Pyrene excimer-formation experiments showed a peptide-induced reduction in lipid lateral mobility. Finally, laurdan fluorescence indicated that peptide binding reduces water penetration below the headgroups region. Comparable effects were observed also in fluorescence experiments performed directly on live bacterial cells. By contrast, the fatty acyl chain order parameters detected by deuterium NMR spectroscopy remained virtually unaffected by addition of the peptides. The apparent discrepancy between the two techniques confirms previous sporadic observations and is discussed in terms of the different characteristic times of the two approaches. The perturbation of membrane dynamics in the ns timescale, indicated by the multiple fluorescence approaches reported here, could contribute to the antimicrobial activity of AMPs, by affecting the function of membrane proteins, which is strongly dependent on the physicochemical properties of the bilayer.

Abbreviations: AMP, antimicrobial peptide; CF, 5,6-carboxyfluorescein; DPH, diphenylhexatriene; NBD-PE, L-α-phosphatidylethanolamine-N-(7-nitro-2-1,3-benzoxadiazol-4-yl); PEG-PE, (1,2-distearoyl-*sn*-glycero-3-phosphoethanolamine-N-[methoxy(polyethylene glycol)-2000]); POPC, 1-palmitoyl-2-oleoyl-*sn*-glycero-phosphocholine; POPG, 1-palmitoyl-2-oleoyl-*sn*-glycero-3-[phospho-rac-(1-glycerol)]; Pyr-PC, 1-palmitoyl-2-(1-pirenedecanoyl)-*sn*-glycero-3- phosphocholine; Pyr-PG, 1-palmitoyl-2-(1-pyrenedecanoyl)-*sn*-glycero-3-phosphoglycerol.

* Corresponding author at: Department of Chemical Science and Technology, University of Rome Tor Vergata, via della Ricerca Scientifica, 1, Rome 00133, Italy.
E-mail address: stella@uniroma2.it (L. Stella).

[1] Current address: IRBM Science Park, 00071 Pomezia RM, Italy.
[2] Current address: Sealed Air Corporation, Via Trento, 7, 20017 Rho MI, Italy.

https://doi.org/10.1016/j.bpc.2023.107060
Received 11 March 2023; Received in revised form 25 May 2023; Accepted 2 June 2023
Available online 8 June 2023

1. Introduction

Antimicrobial peptides (AMPs), also termed host defense peptides, are short amino-acidic sequences produced by most organisms as a defense against pathogens. They have a broad spectrum of activity and are usually bactericidal. Most of them target bacterial membranes, perturbing bilayer permeability [1]. Due to their mechanism of action, fast killing activity, and good selectivity for pathogen versus host cell membranes, AMPs are considered a promising class of compounds to fight the pressing medical problem of antibiotic-resistant infections [2].

Although AMPs are characterized by no conserved sequence motifs, most of them are short, cationic and amphipathic. They usually cause leakage of bacterial membranes by accumulating on their external surface, inserting below the lipid headgroups, parallel to the membrane surface, and perturbing the surface tension of the outer lipid leaflet. When a threshold of bound peptides is reached, defects are formed, to release the accumulated stress. This mechanism of action is commonly termed the "carpet" model, since the threshold for defect formation requires a high coverage of the bilayer surface by bound peptides [3,2].

In an alternative mechanism of pore formation, called "barrel-stave", peptides bind to the membrane surface, then insert in a transbilayer orientation, aggregate like the staves in a barrel, forming pores in the bilayer. In this case, the threshold of membrane-bound peptides required for pore formation can be lower than what is needed for peptides acting according to the carpet mechanism. This mechanism applies only to peptides which are not strongly cationic, and it has been conclusively demonstrated only for peptides belonging to the peptaibiotic family, most notably alamethicin, at least for some lipid compositions [4,2,5].

Peptide accumulation on the membrane surface or insertion into the bilayer can conceivably cause other effects on bilayer properties, in addition to, or even before the formation of pores, or defects. For instance, Richard Epand has first proposed that perturbation of the lateral organization of membranes, due to clustering of anionic lipids by cationic AMPs, can contribute to their antimicrobial activity [6–11,12,13]. More generally, Hans-Georg Sahl proposed that AMPs could lead to bacterial killing by perturbing the structural and dynamical properties of the bilayer, which are essential for the proper function of membrane-bound proteins, acting like "sand in a gearbox" [14]. Indeed, finely tuned dynamical properties of cell membranes are critical in maintaining the viability of bacterial cells and their metabolic functions, as shown by a process termed homeoviscous adaptation: when the external conditions, such as temperature, change, bacteria modify the lipid composition of their membranes, in order to maintain the proper viscosity [15,16,17,18,19,20,21,22]. Inadequate membrane fluidity interferes with essential complex cellular processes including cytokinesis, envelope expansion, chromosome replication/segregation and maintenance of membrane potential [23].

In this work, we systematically assessed the "sand in a box" hypothesis, by focusing on two representative AMPs, PMAP-23 and alamethicin, whose sequences are shown in Scheme 1.

PMAP-23 is a cationic, amphipathic, helical peptide, belonging to the cathelicidin family. It has antimicrobial activity against Gram-positive and Gram-negative bacteria, fungi, protozoa and viruses, but at the same time this peptide is not toxic towards eukaryotic cells [24,25,26]. The mechanism of membrane permeabilization of PMAP-23 has been extensively characterized and demonstrated to conform to the carpet model: the peptide binds to the membrane surface, parallel to it, and causes the formation of pores when a high surface coverage is reached [3,27,28,29,30,31].

PMAP-23	**RIIDLLWRVRRPQKPKFVTVWVR**
Alamethicin F50/5	**AcUPUAUAQUVUGLUPVUUQQFol**

Scheme 1. Sequences of the studied peptides. Hydrophobic, basic and acidic residues are colored in green, blue and red, respectively. Ac = acetyl, U = 2-aminoisobutyric acid, Fol = phenylalaninol.

Alamethicin is a member of the peptaibiotics group of AMPs, a class of nonribosomally synthesized peptides which are characterized by a C-terminal 1,2-amino alcohol, an acylated N-terminus, and a high content of non-proteinogenic residues, such as the α-aminoisobutyric acid (Aib) [32]. The substitution of the H atom on the C_α of Aib with a methyl group reduces the conformational freedom of the amino acid, thus favoring a helical folding of these peptides [33,34]. Alamethicin is active against Gram-positive bacteria and fungi [35,36], but its efficacy against Gram-negative bacteria is reduced, probably because of the lipopolysaccharide (LPS) layer present in the outer membrane, which constitutes a strong barrier against hydrophobic molecules such as peptaibiotics. However, the peptide is also cytotoxic towards mammalian cells [32]. Alamethicin is the prototype of peptides forming pores according to the barrel-stave model [37,38,39], and thus in this work it was selected to represent AMPs acting according to this mechanism. The evidence on the mechanism of pore formation by alamethicin is based on single channel conductance traces and other biophysical data [40,41,42,43,44]. Indeed, solid-state NMR (ssNMR) experiments demonstrated transmembrane (TM) alignments of alamethicin helices in phosphocholine lipids, at elevated peptide to lipid (P/L) ratios [45,46,47,48]. However, it should be noted that alignments parallel to the membrane surface have also been observed when reconstituted into POPE/POPG membranes (3/1 molar ratio) at P/L 1/50 [49]. Therefore, an equilibrium between an in-planar and TM states can be present also for this very hydrophobic peptide, albeit a preferential TM alignment seems to predominate [50,51].

Fluorescence spectroscopy is one of the few experimental techniques that allows the investigation of dynamic phenomena occurring in the nanosecond timescale. Therefore, it is a perfect tool to examine the effects of peptide/membrane association on bilayer dynamics [52]. In this work, we systematically analyzed different aspects, including membrane fluidity, water penetration and lipid lateral mobility, using several fluorophores, located at different depths in the bilayer [53,54,55]. Our fluorescence studies were performed both in model membranes and in live bacterial cells. In addition, we studied peptide effects on lipid order with the complementary technique of ssNMR of membranes containing chain-deuterated lipids. In this approach, the quadrupole splitting of each acyl chain segment directly reflects the motional order parameters within the hydrophobic region and thereby contain both structural and dynamic information [56,57]. The direct comparison of the two approaches allowed us to address the consistency of the pictures on membrane order and dynamics obtained by two experimental methods that sample very different time scales (ns for fluorescence, μs for NMR) [58,59].

2. Materials and methods

2.1. Materials

POPG (1-palmitoyl-2-oleoyl-*sn*-glycero-3-[phospho-rac-(1-glycerol)]), POPC (1-palmitoyl-2-oleoyl-*sn*-glycero-phosphocholine), NBD-PE (L-α-phosphatidylethanolamine-N-(7-nitro-2-1,3-benzoxadiazol-4-yl)), and PEG-PE (1,2-distearoyl-*sn*-glycero-3-phosphoethanolamine-N-[methoxy(polyethylene glycol)-2000]) were purchased from Avanti Polar Lipids (Alabaster, Al); Pyr-PC (1-palmitoyl-2-(pyrene-1-yl)decanoyl-*sn*-glycero-3-phosphocholine) and Pyr-PG (1-palmitoyl-2-(pyrene-y-yl)decanoyl-*sn*-glycero-3-phosphoglycerol) were obtained from Sigma Aldrich (St. Louis, MO); DPH (diphenylhexatriene) and laurdan (2-(dimethylamino)-6-dodecanoylnaphthalene) were purchased from Fluka (St. Louis, MO). Spectroscopic-grade chloroform and methanol (Carlo Erba, Milano, Italy) were used. Triton X-100 was purchased from Acros (Geel, Belgium).

PMAP-23 was purchased by AnyGen (Republic of Korea), and had a purity of 97.3%, as determined by HPLC (expected mass 2962.6 Da, measured mass found 2963.0 Da). The synthesis and characterization of

alamethicin has been described previously [60].

2.2. Apparatus

Steady-state fluorescence experiments were carried out with a Fluoromax-4 fluorimeter (Horiba, Edison, NJ). Time-resolved measurements were performed with a Lifespec-ps fluorometer (Edinburg instrument, Edinburgh, UK). Sample temperature was controlled to 25.0 °C (within 0.1 °C) with a termostatted water bath.

2.3. Liposome preparation

Large unilamellar vesicles were prepared by dissolving in a 1:1 (vol/vol) chloroform/methanol mixture POPC/POPG lipids (2:1 molar ratio), and the appropriate fluorophore (laurdan, NBD-PE, DPH, Pyr-PG, or Pyr-PC), or PEG-PE (2 mol% with respect to the total lipid concentration), when needed. The fluorophore was at a ratio of 1% with respect to the total lipids, with the exception of Pyr-PG and Pyr-PC, which were 3%. The solvents were evaporated under reduced argon atmosphere until a thin film was formed. Complete evaporation was ensured by applying a rotary vacuum pump for at least 2 h. The lipid film was hydrated with phosphate buffer 10 mM (pH 7.4) containing NaCl 140 mM and EDTA 0.1 mM, or a 30 mM 5,6-carboxyfluorescein (CF) solution for the leakage experiments. The liposome suspension was vigorously stirred and 10 freeze and thaw cycles were performed. The suspension was extruded through two stacked polycarbonate membranes with 100 nm pores for 31 times, to ensure a narrow size distribution [61]. Liposomes hydrated with the CF solution were separated from unencapsulated dye by gel filtration on a Sephadex G-50 medium column. The final lipid concentration was determined by the Stewart method [62].

2.4. Liposome leakage

Perturbation of membrane permeability was determined by measuring the fractional release of the CF fluorophore entrapped inside liposomes. This quantity can be measured directly by the increase in fluorescence intensity caused by the reduction in CF self-quenching. The fractional release was calculated as follow:

$$R = \frac{F - F_{0\%}}{F_{100\%} - F_{0\%}}, \tag{1}$$

where $F_{0\%}$ is the fluorescence of the probe before peptide addition, and $F_{100\%}$ is the intensity after complete disruption of the vesicles caused by the addition of Triton X-100 (1 mM). The release kinetics was recorded with an FluoroMax-4 fluorimeter with excitation and emission wavelengths of 520 nm (bandwidth 0.2 nm) and 490 nm (bandwidth 1.5 nm), respectively.

2.5. Steady-state and time-resolved anisotropy

Perturbation of membrane dynamics caused by peptides was analyzed by experiments of steady-state and time-resolved anisotropy of two different probes, DPH and NDB-PE. In both cases, probe to phospholipids molar ratio was fixed to 1:100.

For DPH steady-state anisotropy, the experimental conditions were set as follow: excitation wavelength 372 nm, emission wavelength 450 nm, bandwidth 4 nm and 385 nm cut-off filter. For NBD-PE static anisotropy, the excitation wavelength was set to 460 nm, emission 530 nm, bandwidth 4 nm and 495 nm cut-off filter. Each experimental point was determined nine times, and the mean value was reported.

Time-resolved anisotropy experiments were performed with the time-correlated single photon counting technique. The excitation source was a laser at 440 nm. The emission bandwidth was set at 8 nm, and the other parameters were the same of steady-state anisotropy.

2.6. Generalized polarization

Spectra of laurdan-labelled liposomes were recorded from 400 nm to 520 nm (excitation wavelength 364 nm, 2 nm bandwidth both in excitation and emission). The generalized polarization was calculated as follow:

$$GP = \frac{F_{435\ nm} - F_{500\ nm}}{F_{435\ nm} + F_{500\ nm}} \tag{2}$$

where F_λ is the fluorescence intensity relating to a specific emission wavelength λ.

2.7. Lipid lateral mobility

Liposomes were labelled with the fluorescent probe pyrene covalently linked to the hydrocarbon chain of phospholipids. Liposome with two different compositions were prepared: POPC/POPG/Pyr-PG (66:30:3 molar ratio) and POPC/POPG/Pyr-PC (63:33:3 molar ratio).

Pyrene fluorescence spectra (370–700 nm) were recorded at increasing peptide concentrations (excitation wavelength 328 nm, integration time 0.1 s, excitation and emission bandwidths 1 nm and 1.5 nm respectively). Excimers over monomer fluorescence intensity was measured as the ratio between fluorescence values at 475 nm and 397 nm.

With PMAP-23, Förster resonance energy transfer was exploited to selectively excite the pyrene fluorophores surrounding peptide molecules, by exciting the tryptophan residues on the peptide chain (excitation wavelength 280 nm, integration time 0.5 s, excitation and emission bandwidths 1 nm and 1.5 nm, respectively).

2.8. Experiments with bacteria

Escherichia coli ATCC 25922 was grown in Luria-Bertani (LB) medium at 37 °C in an orbital shaker until a mid-log phase, which was aseptically monitored by absorbance at 590 nm (A590 nm = 0.8) with an UV-1700 Pharma Spec spectrophotometer (Shimadzu, Tokyo, Japan). The cells were subsequently centrifuged and washed eight times with buffer A (5 mM HEPES, pH = 7.3, 110 mM KCl, 15 mM glucose) to remove traces of LB medium. Previous studies showed that in this minimal culture medium, bacteria remain vital, but do not multiply, thus maintaining a constant density of live cells, for at least 6 h at 25 °C and 2 h at 37 °C [29].

Bacterial cells, at a density of 4.5×10^8 CFU/mL, were incubated with the appropriate fluorescent probe for 30 min. This incubation time ensured stabilization of the signal (anisotropy, GP or E/M ratio). The cell density was select to ensure adequate membrane partitioning of the probe and, at the same time, to avoid instrumental artifacts due to light scattering [29]. Laurdan and DPH were added from methanolic stock solution, at a final concentration of 1 μM, while pyrene concentration was 2.5 μM, to enhance excimer formation. Subsequently, increasing concentrations of the peptide PMAP-23 were added. Incubation and measurements were carried out at 37 °C.

Finally, the bactericidal activity of PMAP-23 was assessed against *E. coli* ATCC 25922 in buffer A. Bacterial cells (4.5×10^8 CFU/mL) were incubated at 37 °C and 800 rpm with different concentrations of PMAP-23 or methanol (peptide solvent, as control). After 2 h, aliquots were spread on LB-agar plates for the CFU counting. The fraction of surviving bacterial cells was calculated with respect to the control samples.

2.9. Sample preparation for ssNMR spectroscopy

Samples were prepared by dissolving 1 mg of deuterated lipids (POPC-d_{31}, POPG-d_{31}, or POPE-d_{31}, or POP-d or POPG-d_{31}) and appropriate amounts of the second lipid component and of peptide in methanol/chloroform (1:1 by volume). The solvent was evaporated under a

stream of nitrogen and then in a high vacuum, overnight, to form a film on the walls of the small glass tube (6 mm outer diameter). The sample was then resuspended in 100 mM Tris buffer (pH 7.4) by vortexing and bath sonication, followed by 3 freeze/thaw cycles. The water content was set to 81% (mass of water relative to the total mass of lipids and water system).

The glass tube with the sample inside was then inserted into the solenoidal coil of a static NMR probe and investigated by ssNMR spectroscopy.

2.10. SsNMR spectroscopy

Deuterium ssNMR spectra were recorded using a quadrupolar echo pulse sequence [63] with a repetition delay of 0.3 s, an echo time of 100 μs, a dwell time of 0.5 μs and a B_1 field of 45 kHz. The spectra were referenced relative to ^2H_2O (0 Hz). An exponential apodization function corresponding to a line broadening of 100 Hz was applied before Fourier transformation. The temperature was set to 25 °C for POPC/POPG 2/1 and to 37 °C for POPE/POPG 3/1. The deuterium order parameters are analyzed following [51].

2.11. Deuterium order parameters

The deuterium order parameters (S_{CD}) of the CD_2 and CD_3 groups was calculated according to: $S^i_{CD} = \frac{4}{3}\frac{h}{e^2qQ}\Delta^i\upsilon$, where $\Delta^i\nu$ is the quadrupolar splitting of segment i and (e^2qQ/h) is the static quadrupole coupling constant (167 kHz) for C—D deuterons [64]. When establishing order parameter profiles, based on early studies of pure lipid bilayers labelled with $^2H_2$—C at individual segments one at a time, it is assumed that the order parameters diminishes in a continuous fashion from the membrane interface to the membrane interior.

3. Results

3.1. Perturbation of membrane permeability

Pore formation is the most well-characterized effect of the interaction of AMPs with phospholipid membranes, and is usually related to their microbicidal activity. To define the range of peptide concentrations where this phenomenon takes place, and to relate it to other possible effects on the membrane, the leakage induced by PMAP-23 and alamethicin was studied through the use of carboxyfluorescein (CF) entrapped into POPC/POPG 2:1 liposomes. This lipid composition was used as a simple model of the anionic nature of bacterial membranes [65]. Vesicles (lipid concentration 50 μM) were thus titrated with increasing concentrations of peptide and the release kinetics of the fluorescent probe was recorded. Fig. 1 shows the fraction of CF released 20 min after peptide addition as a function of peptide concentration. The gray shaded areas indicate the concentration range where the peptide pore-forming activity goes approximately from 0% to 100%.

Alamethicin is about ten times more active than PMAP-23, and the peptide-concentration dependence of its activity is steeper. These findings are consistent with the different mechanisms of pore formation of the two peptides. The carpet mechanism of PMAP-23 requires substantial membrane coverage for bilayer defect formation. On the other hand, peptide aggregation in the membrane is involved in the barrel-stave mechanism of alamethicin, providing a possible explanation for the observed highly cooperative behavior.

In order to compare PMAP-23 and alamethicin activities, the bilayer-bound peptide concentration would be a more relevant parameter than the total peptide in the sample. However, in the following sections of this article, we will be comparing pore-forming activity to other membrane-perturbing effects. Since the experimental conditions (and particularly the lipid concentration) will remain unchanged, all fluorescence spectroscopy datasets for each individual peptide will be directly comparable, even considering the total peptide concentration.

3.2. Perturbation of membrane fluidity and order: steady-state anisotropy

Steady-state fluorescence anisotropy is determined by the speed and amplitude of the rotational motions of a fluorophore during its excited-state lifetime. Slow (compared to the lifetime) and/or limited motions correspond to high anisotropy values (with the maximum, limiting value being 0.4), while fast and wide rotations yield anisotropy values close to zero. Molecular motions are obviously influenced by the viscosity of the fluorophore's environment, and anisotropy measurements can be used to determine the local viscosity and packing of a lipid membrane. Therefore, we exploited fluorescence anisotropy measurements to determine the peptide effects of on membrane fluidity, by using two probes inserted at different depths into the lipid bilayer: NBD-PE and DPH. In NBD-PE, the fluorophore is attached to the phospholipid headgroup, and its position in the bilayer is therefore very superficial. Depth-dependent quenching (DDQ) experiments determined an average position of the probe at about 19–20 Å from the bilayer center [53,66], and this value is in agreement with previous estimates based on FRET experiments [67]. A more detailed distribution analysis of DDQ data

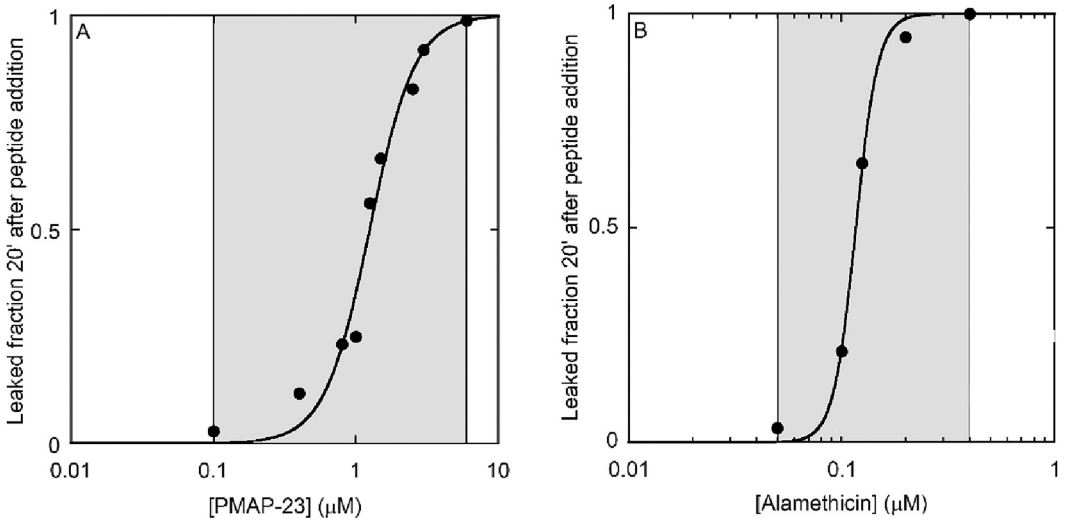

Fig. 1. Fraction of CF released 20 min after the addition of PMAP-23 (A panel) or alamethicin (B panel). Lipid concentration 50 μM, liposome composition: POPC/POPG 2:1 (molar ratio). The gray shaded areas represent the concentration range in which the peptide pore-forming activity goes approximately from 0% to 100%.

indicated that the probe can sample a rather wide distribution of positions, with a maximum at about 15 Å from the bilayer center, and molecular dynamics simulations are consistent with this finding [68], showing the possibility of a downward bending of the phosphoethanolamine group, with NBD insertion slightly below the headgroups [69]. DPH position in the membrane has been characterized by several techniques. DDQ experiments determined an average position of 7.8 Å from the center of a PC membrane [55]. Recent MD simulations [70,71,72] are consistent with this finding but indicate a distribution of locations in the hydrophobic core of the bilayer. Neutron [73] indicate that DPH molecules can be located also closer to the membrane surface, although the population of this position was not quantified. Notwithstanding the complex behaviors indicated by these data, on average the hydrophobic DPH definitely locates much deeper in the bilayer than the polar NBD moiety, attached to a phospholipid headgroup.

Both peptides caused an increase in anisotropy (Figs. 2 and 3), indicative of a decreased mobility of the probes. The same effect was observed for both labels, indicating a global, rather than local effect of the peptides on membrane properties. This finding is rather surprising, considering that the peptides were shown to cause membrane defects, which might naively be associated with an increase in membrane disorder and mobility.

For both peptides, the effects on membrane fluidity started at a concentration of about 1 μM. However, in the case of PMAP-23 this corresponds to the concentrations causing bilayer leakage, while in the case of alamethicin pores are formed already at much lower concentrations.

3.3. Perturbation of membrane fluidity and order: time-resolved anisotropy

As discussed above, an increase in steady-state anisotropy could be caused by a decrease in the speed and/or amplitude of the fluorophore's rotational motions. In addition, steady-state anisotropy could vary also due to changes in the excited state lifetime. To better clarify these aspects, time-resolved anisotropy experiments were performed, in the absence of peptides, and with a PMAP-23 concentration able to cause a leakage close to 100% (Fig. 4).

The results of data analysis are reported in Table 1. Data were satisfactorily fitted by a biexponential decay:

$$r(t) = r_0\left(f_1 e^{-t/\phi_1} + f_2 e^{t/\phi_2} + 1 - f_1 - f_2\right) \quad (3)$$

where r_0 is the limiting anisotropy and ϕ_1 and ϕ_2 are the rotational correlation times. The fraction of residual anisotropy (which quantifies how hindered are the motions) can be calculated as

$$f_\infty = 1 - f_1 - f_2 \quad (4)$$

An average rotational correlation time can be calculated by the following equation:

$$\langle\phi\rangle = (f_1\phi_1 + f_2\phi_2)/(f_1 + f_2) \quad (5)$$

The biexponential trend of the anisotropy decays indicates that the probe motions cannot be described as a simple rotation. Peptide addition caused an increase in both the average rotational correlation time and in the fraction of residual anisotropy, indicating that the probe motions are slower and more hindered.

3.4. Water penetration

Phospholipid membranes constitute a barrier for the diffusion of polar solutes. However, some water molecules can percolate in the headgroups region. The degree of water penetration is strictly correlated to the fluidity of the membrane, for instance, it increases dramatically during the thermotropic phase transition of lipid bilayers from the liquid ordered to the liquid disordered phase. The fluorescent probe laurdan can be exploited to quantify water penetration in the bilayer, because its fluorescence spectrum is very sensitive to the environment polarity, showing a red shift of approximately 50 nm when water molecules surround the naphthalene moiety, compared to when the environment is apolar. Its average position in the bilayer, as determined by DDQ experiments, is at about 10–11 Å from the bilayer center [74,75]. Molecular dynamics simulations are consistent with these results but show a distribution of positions in the bilayer [76]. Importantly, it has been demonstrated that peptide or protein binding to the membrane, per se, does not perturb the laurdan spectrum [77], and that this probe is completely bound to the membrane, at the lipid concentrations used in the present study [78]. A common method to quantify this spectral shift is to calculate a parameter called generalized polarization (GP, see the methods section for the definition), which has positive values when the spectrum is blue shifted (apolar environment), and negative values when it is red-shifted (polar environment).

Fig. 5 illustrates the trend of GP as a function of peptide concentration. For both peptides, the data indicate a reduction of the degree of water penetration inside the bilayer, in agreement with the membrane stiffening shown by anisotropy measurements. Once again, the effect takes place at similar concentrations for both peptides (above 1 μM), but for PMAP-23 these values correspond to those causing membrane

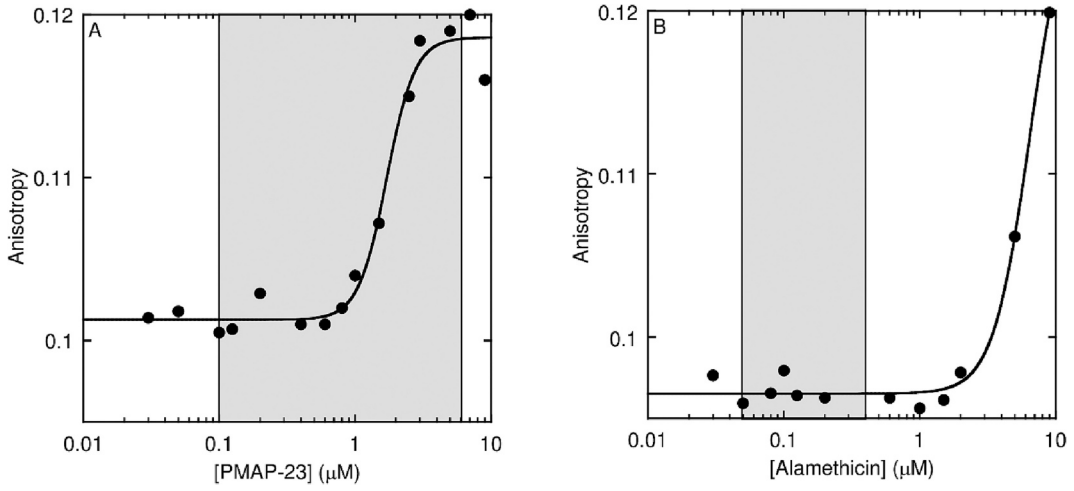

Fig. 2. Steady-state anisotropy of DPH in liposomes, during titration with PMAP-23 (A) or alamethicin (B). $\lambda_{ex} = 372$ nm, $\lambda_{em} = 385$ nm. Lipid concentration 50 μM, liposome composition: POPC/POPG (2:1 molar ratio), probe to phospholipids molar ratio 1:100.

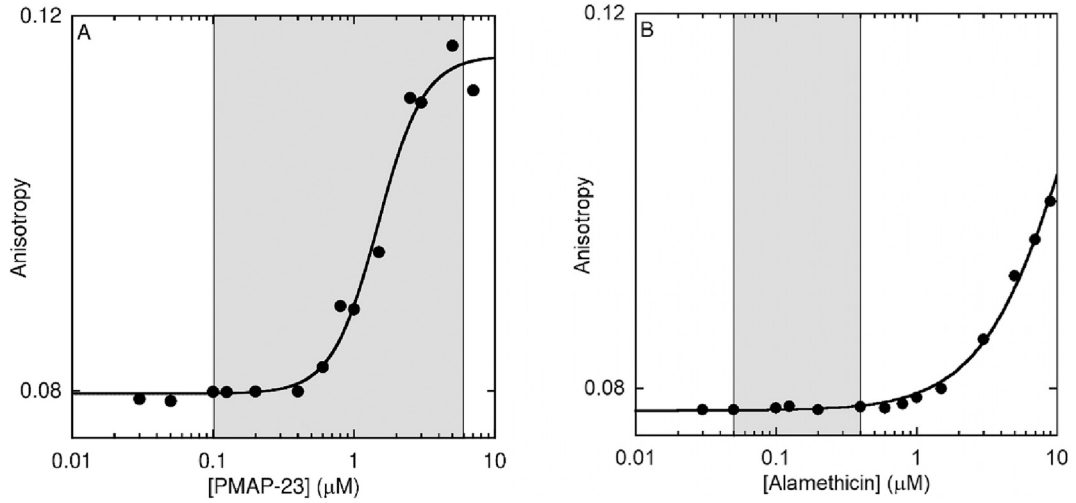

Fig. 3. Steady-state anisotropy of NBD-PE inserted into liposomes, during titration with PMAP-23 (A) or alamethicin (B). λ_{ex} = 460 nm, λ_{em} = 530 nm. Lipid concentration 50 μM, liposome composition: POPC/POPG (2:1 molar ratio), probe to phospholipids molar ratio 1:100.

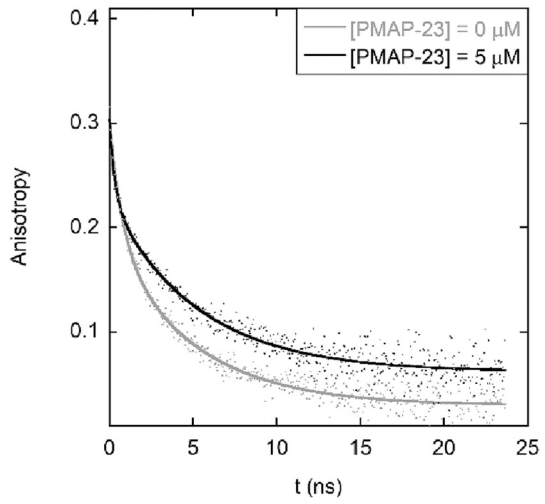

Fig. 4. Time-resolved anisotropy decay of the probe NBD-PE inserted into liposomes (probe to phospholipids molar ratio 1:100) before and after the addition of PMAP-23 (5 μM). λ_{ex} = 440 nm, λ_{em} = 530 nm. Lipid concentration 50 μM, liposomes composition: POPC/POPG (2:1 molar ratio).

Table 1
Parameters of biexponential fits of NBD-PE anisotropy decays.

	[PMAP-23] = 0	[PMAP-23] = 5 μM
r_0	0.302 ± 0.004	0.303 ± 0.005
ϕ_1(ns)	4.9 ± 0.3	5.3 ± 0.2
f_1	0.54 ± 0.02	0.55 ± 0.01
ϕ_2(ns)	0.76 ± 0.08	0.33 ± 0.05
f_2	0.36 ± 0.02	0.25 ± 0.01
$<\phi>$ (ns)	3.2 ± 0.2	3.8 ± 0.1
f_∞	0.10 ± 0.02	0.20 ± 0.04
χ_r^2	0.7	0.7

leakage, while for alamethicin they are higher than those causing pore formation.

3.5. Lipid lateral mobility

The lateral diffusion of phospholipids in the plane of the bilayer is another aspect that is worth analyzing to further investigate peptide effects on membrane dynamics. The peculiar photophysical properties of pyrene were exploited to investigate this motion. When an excited and a ground-state pyrene molecule come in contact, a complex called excited-state dimer (or excimer) can form. This species is fluorescent, too, with an emission spectrum that is very different from that of the monomer and shifted to longer wavelengths. Excimer formation depends on the local concentration of pyrene molecules, but also on their mobility, since it is diffusion-limited and depends on the probability of diffusional encounter of two pyrene molecules (one of which is excited), during the duration of the excited-state lifetime. Therefore, it can be used to get information concerning the lateral diffusion of pyrene-labelled lipids, by measuring the ratio between the intensities of the excimer and monomer emission bands, peaked at 475 nm and 397 nm, respectively (E/M ratio). For this purpose, liposomes including lipids labelled with pyrene on the end of one of their tails (Pyr-PC or Pyr-PG, depending on the heagroup) were employed. In this case, the pyrene moieties are so close to the bilayer center that fluorophores from opposing leaflets can dimerize [79].

PMAP-23 addition to liposomes containing zwitterionic pyrene-labelled phospholipids (Pyr-PC) caused a reduction in the EM ratio (Fig. 6), indicating a decrease in the lateral mobility of phospholipids. A slightly different trend was observed for PMAP-23 when the pyrene-labelled lipids were anionic (Pyr-PG): in the range of low peptide concentrations, an increase in the E/M ratio was found, but the trend reversed when the peptide concentration increased. A possible explanation of this behavior might be related to the cationic nature of PMAP-23, which could drive its preferential interaction with anionic phospholipids. Clustering of POPG by the peptide could thus increase the local concentration of Pyr-PG, favoring the formation of excimers. However, when the peptide concentration raises, the reduction in lipid lateral mobility, observed also with POPC, probably becomes the predominant effect, leading to a reduction in excimer emission. This interpretation was supported also by experiments performed by exploiting the energy transfer from the tryptophan residues of the peptide chain to pyrene, and thus specifically analyzing the region surrounding PMAP-23. In this case, the trend of the E/M ratio was similar, but the initial increase in the E/M ratio for Pyr-PG was enhanced.

In the case of alamethicin, for both labelled lipids, a decrease in excimer formation was observed for concentrations higher than 1 μM. As in the case of anisotropy and laurdan experiments, this value is comparable to the PMAP-23 concentration where perturbation of membrane dynamics begins, but for alamethicin is much higher than the range where the peptaibol causes membrane leakage.

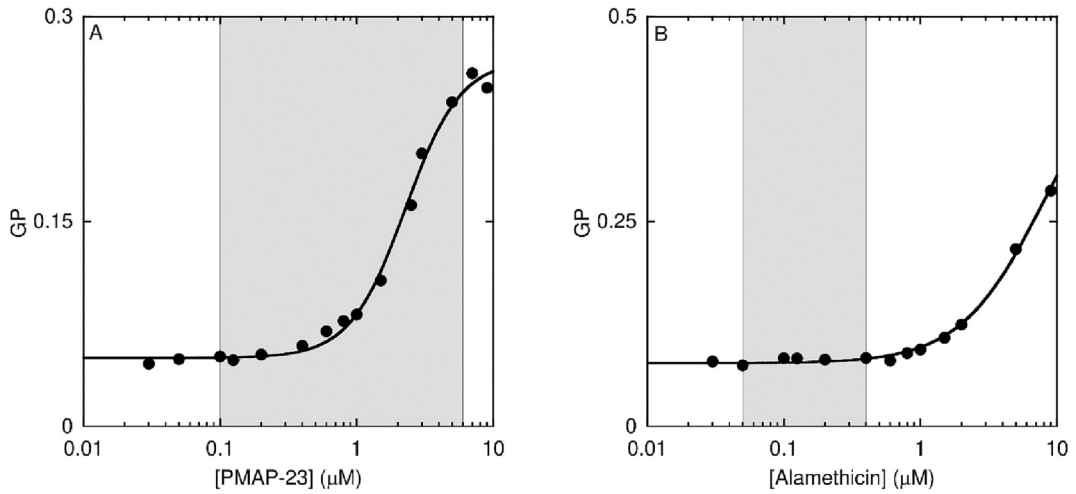

Fig. 5. Generalized polarization of laurdan inserted into liposomes at increasing concentrations of PMAP-23 (A) and alamethicin (B). Lipid concentration 50 μM, liposome composition: POPC/POPG (2:1 molar ratio), laurdan to phospholipids molar ratio 1:100.

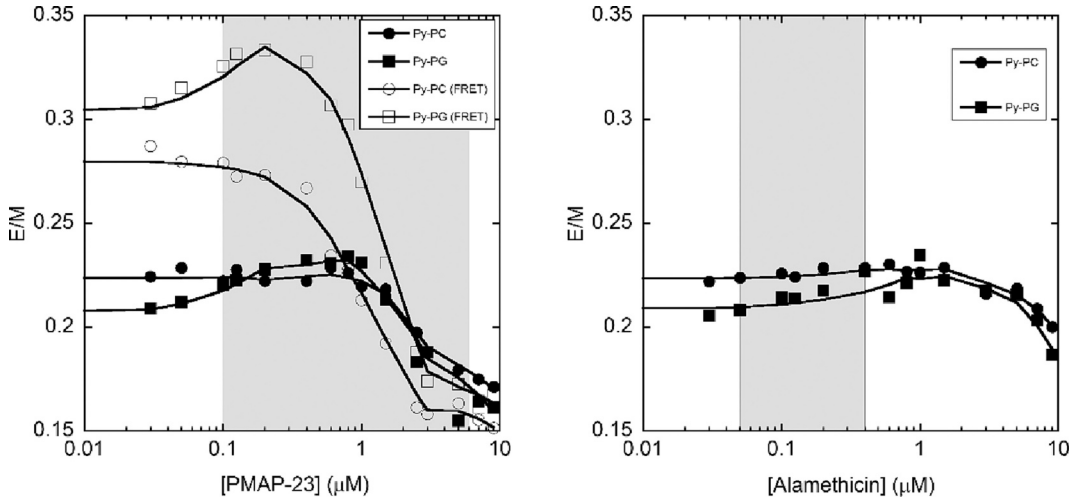

Fig. 6. Excimer over monomer emission intensity ratio E/M (λ_{ex} = 328 nm, λ_{em} = 475 nm and 397 nm respectively) as a function of peptide concentration (PMAP-23 left panel, alamethicin right panel). Lipid concentration 50 μM, liposome composition: POPC/POPG (2:1 molar ratio). The pyrene probe was covalently bound to phospholipid hydrocarbon chains with different headgroups: Pyr-PG (squares) and Pyr-PC (circles), 3% of total lipids. In the case of PMAP-23, empty symbols refer to experiments performed by exciting pyrene through FRET from the Trp residues of the peptide chain (λ_{ex} = 280 nm).

3.6. Vesicle aggregation

Following addition of PMAP-23 to the liposome suspension, some turbidity appeared in the sample, particularly at high peptide concentrations. This is a common observation with cationic peptides and is due to the formation of vesicle aggregates caused by the neutralization of the membrane surface by bound peptides [80,81]. The turbidity caused by vesicle aggregation was quantified by measuring the apparent absorbance at 600 nm of the liposome suspension in the presence of increasing peptide concentrations. Liposome aggregation was negligible in the case of alamethicin (data not shown). On the contrary, PMAP-23 (Fig. 7), showed an increase in the scattered light with the addition of the peptide to the lipid mixture. This effect was significant in the same concentration range where the perturbation of the membrane dynamics (and vesicle leakage) caused by PMAP-23 was observed. It is thus reasonable to question whether all the variations in membrane dynamics reported in the previous sections arise from the peptide-induced perturbations of the bilayer, or are simply a consequence of vesicle aggregation, at least in the case of PMAP-23. To clarify this point, vesicle aggregation was inhibited by increasing the steric repulsion between vesicles, preparing liposomes including in the lipid mixture phospholipids derivatized on their headgroup with the hydrophilic polymer polyethylene glycol. This approach essentially eliminated liposome aggregation but did not significantly affect PMAP-23 effects on DPH anisotropy (Fig. 7). Therefore, the possibility that the peptide-induced reduction in membrane fluidity is an artifact arising from vesicle aggregation can be ruled out.

3.7. Perturbation of membrane dynamics in live bacterial cells

To test the biological relevance of the present findings, we measured peptide effects on the dynamics of membranes of live *E. coli* cells, rather than of artificial vesicles. This was possible by incubating the cells with DPH, laurdan or pyrene, which spontaneously insert into bacterial membranes [82,83,84]. In all cases (Figs. 8–10), the peptide effects were similar to those observed in artificial vesicles: an increase in DPH anisotropy (Fig. 8) and laurdan GP (Fig. 9), and an initial rise, followed by a decrease, in pyrene excimer to monomer intensity ratio (Fig. 10).

These findings demonstrate that PMAP-23 affects membrane dynamics also in real, live cells. Interestingly, contrary to what has been

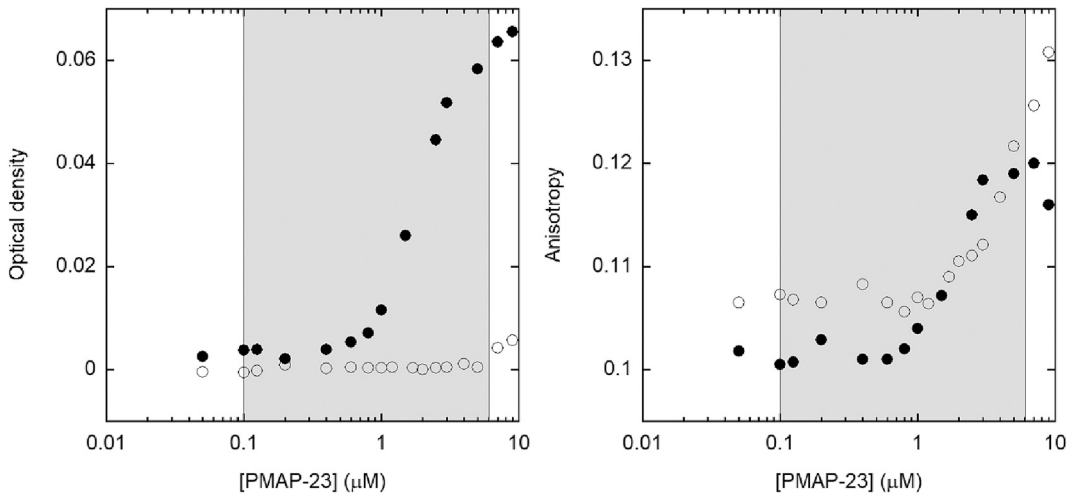

Fig. 7. Optical density of suspension of liposomes of different compositions, measured at 600 nm, during titration with PMAP-23 (left panel), and peptide-induced increase in fluorescence anisotropy of DPH (right panel). Full symbols: POPC/POPG (2:1 molar ratio), open symbols POPC/POPG (2:1 molar ratio) containing 2% of PEG-PE.

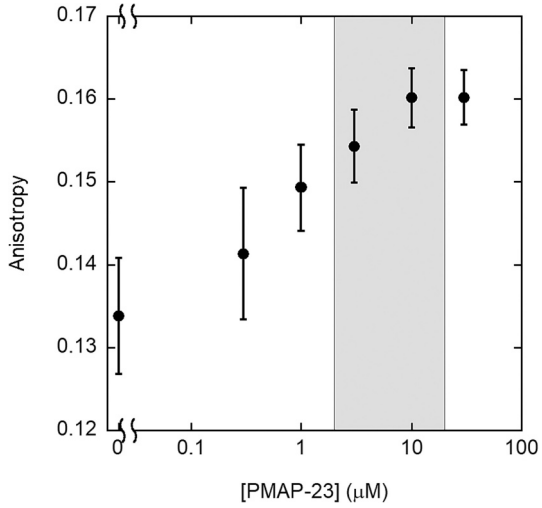

Fig. 8. Effect of PMAP-23 on the membrane dynamics of live *E. coli* cells (cell density 4.5×10^8 CFU/mL), determined by measuring the steady-state anisotropy of DPH (1 μM), in the presence of increasing peptide concentrations. Error bars represent standard errors of triplicate experiments. The shaded gray area indicates the peptide concentration range where bacterial killing goes from 0 to >99.9%.

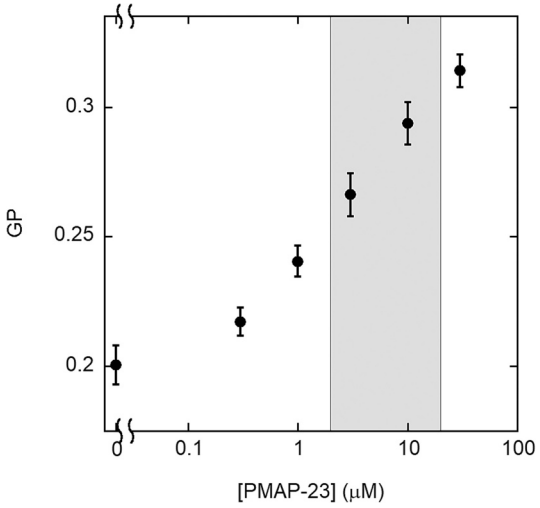

Fig. 9. Effect of PMAP-23 on membrane hydration in live *E. coli* cells (cell density 4.5×10^8 CFU/mL), determined by measuring the generalized polarization (GP) of the laurdan probe (1 μM) in the presence of increasing peptide concentrations. Error bars represent standard errors of triplicate experiments. The shaded gray area indicates the peptide concentration range where bacterial killing goes from 0 to >99.9%.

observed in the case of liposomes, in cells these effects are observed even at concentrations lower than those causing bacterial killing (Figs. 8–10 and Fig. S1).

3.8. Lipid order parameters from ^2H ssNMR spectroscopy

SsNMR is a widely used method to measure membrane order and structure [56,85,57,86]. To better characterize the peptide effects observed in the previous sections, we performed ^2H ssNMR spectroscopy studies for PMAP-23 and alamethicin in POPC/POPG 2/1 liposomes where one of the two phospholipids was fully deuterated at the palmitoyl chain.

In liquid crystalline bilayers where fast rotation along the molecular long axis occurs, each CD_2 segment is associated a quadrupolar powder pattern where the shape, the line width and the quadrupolar splitting are indicators of the average angle of the C—D bond relative to the membrane normal [56]. The spectra are composite of contributions from each CD_2 segment (Fig. 11A, D). For pure lipid bilayers it has been shown that the segments close to the glycerol backbone result in the superposition of spectra with the largest splittings (plateau region). The quadruploar splittings gradually decrease when moving closer to the hydrophobic center with the methyl group exhibiting the narrowest quadrupolar doublet. The spectra can be deconvoluted and an order parameter calculated for each segment (cf. methods section) [56].

Fig. 11 A–C shows the deuterium ssNMR spectra measured from deuterated POPG in POPC/POPG-d_{31} (2/1 molar ratio) liposomes. The spectrum of pure liposomes is shown and compared to recordings in the presence of 2 mol% or 6 mol% of PMAP-23 or of alamethicin (Fig. 11A). An order parameter of 0.20 is observed for the plateau region in agreement with previous publications of related mixtures [87]. From these spectra the order parameters are extracted where the plateau region encompasses segments 2 to 8 of the deuterated POPG palmitoyl chain (Fig. 11B). When the segmental order parameter in the presence of peptide is compared the one obtained from pure lipid the relative order

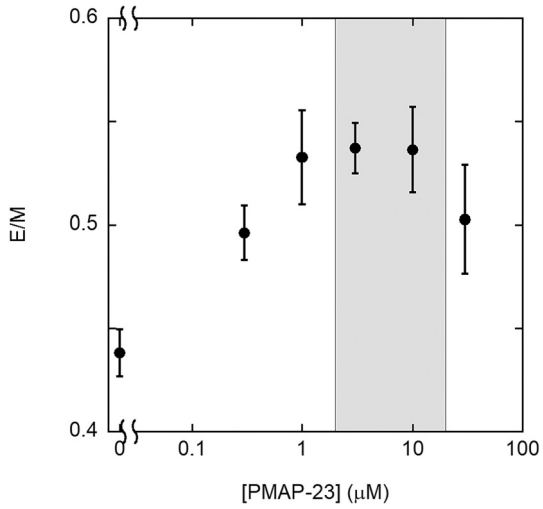

Fig. 10. Effect of PMAP-23 on the lateral mobility of lipids in the membranes of live *E. coli* cells (cell density 4.5×10^8 CFU/mL), determined by measuring the excimer over monomer emission intensity ratio (E/M) of the pyrene probe (concentration 2.5 μM), in the presence of increasing peptide concentrations. Error bars represent the interval of duplicate experiments. The shaded gray area indicates the peptide concentration range where bacterial killing goes from 0 to >99.9%.

parameter is obtained (Fig. 11C). The quadrupolar splittings of the spectra in the absence or in the presence of peptides were surprisingly similar and a relative order parameter of about 1 was obtained in the presence of PMAP-23 or alamethicin (Fig. 11C), indicating the absence of observable peptide effects.

Fig. 11 D—F shows the same series of experiments with the POPC palmitoyl deuterated in the POPC-d_{31}/POPG 2/1 membrane. Again, an order parameter of 0.20 was measured for the plateau region, showing that both lipids mix well under these conditions [87]. Like in the case of the anionic POPG, no significant peptide effects were observed on the order parameter of the zwitterionic lipid (Fig. 11F).

An AMP-induced decrease in the membrane order parameters has been reported in previous ssNMR studies for several peptides, including magainin 2 [87], using POPE/POPG membranes, which mimic the bacterial membrane composition more closely than POPC/POPG. To verify if the lack of significant effects on bilayer order reported above was due to the membrane composition, ssNMR and fluorescence experiments were repeated in POPE/POPG (3/1 molar ratio) bilayers. ssNMR experiments were performed at 310 K, in the presence of 2 mol% PMAP-23. For comparison, magainin 2 was investigated, too. Like PMAP-23, this peptide binds parallel to the bilayer surface [88,89,90]. The plateau region of the deuterium order parameter of the pure lipid bilayers was 0.23 in agreement with previous investigations [87]. Like in the case of POPC/POPG membranes, addition of PMAP-23 to this lipid composition caused very little changes in the palmitoyl order parameters of POPG (Fig. 12A–C) or POPE (Fig. 12D—F) phospholipids. By contrast, magainin 2 induced major perturbations in the membrane packing (Fig. 12). Significant changes in the spectral appearance and a large decrease in the order parameters were observed for both lipids (Fig. 12), albeit more pronounced for the anionic POPG. This observation agrees with previous recordings [87] and is indicative of an increase in gauche isomerizations along the palmitoyl chain [56].

Fig. 13 reports the changes in laurdan generalized polarization induced by PMAP-23 in POPE/POPG liposomes (data regarding POPC/POPG vesicles are reported again, for comparison). Irrespective of the membrane composition, the peptide induces a decrease in water penetration in the bilayer.

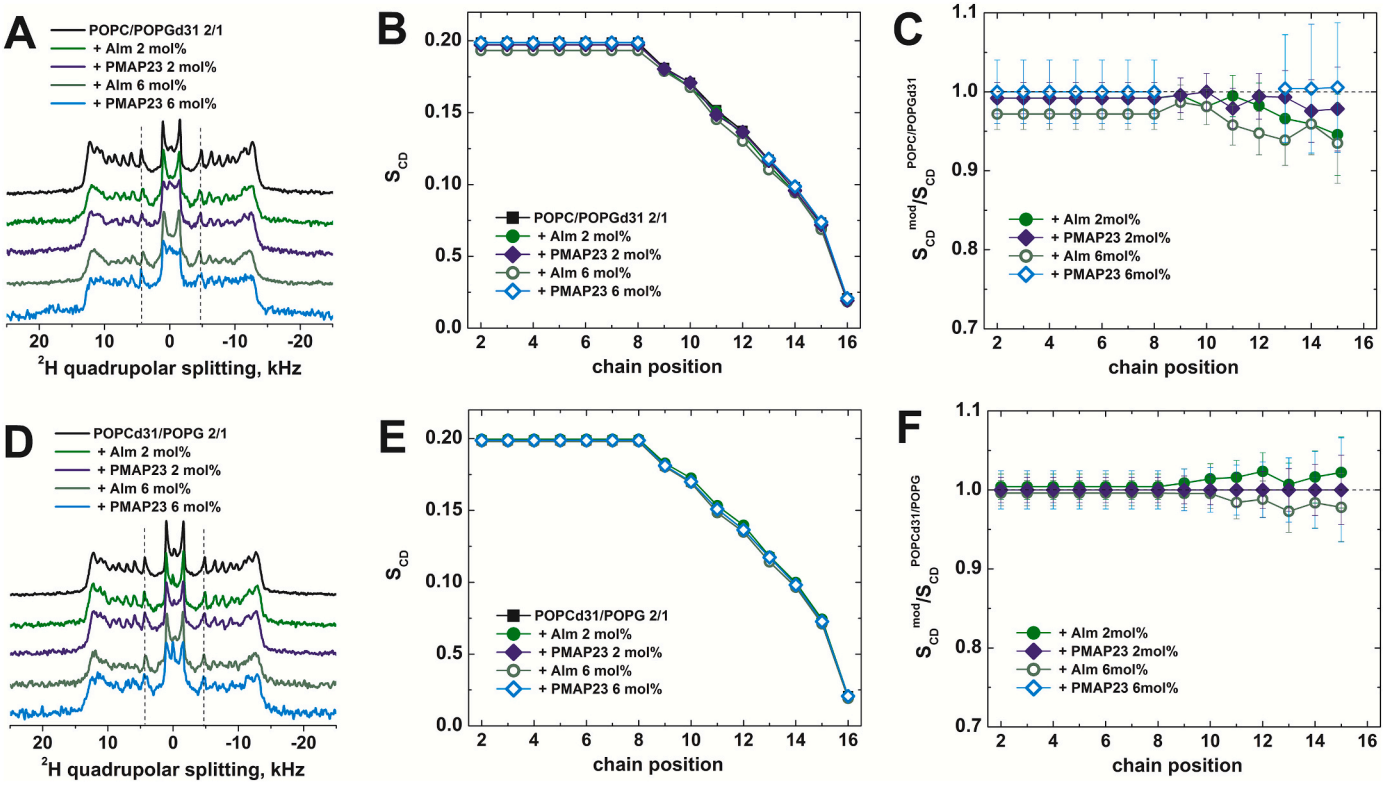

Fig. 11. Deuterium ssNMR spectra of POPC/POPG-d_{31} (2:1 molar ratio) (A-C) and POPC-d_{31}/POPG (2:1 molar ratio) membranes (D—F)in the absence and presence of PMAP-23 or alamethicin. From the ^{2}H ssNMR spectra (A,D), the order parameters (B,E) and relative order parameters (C,F) were calculated for each segment. The temperature was set to 25 °C.

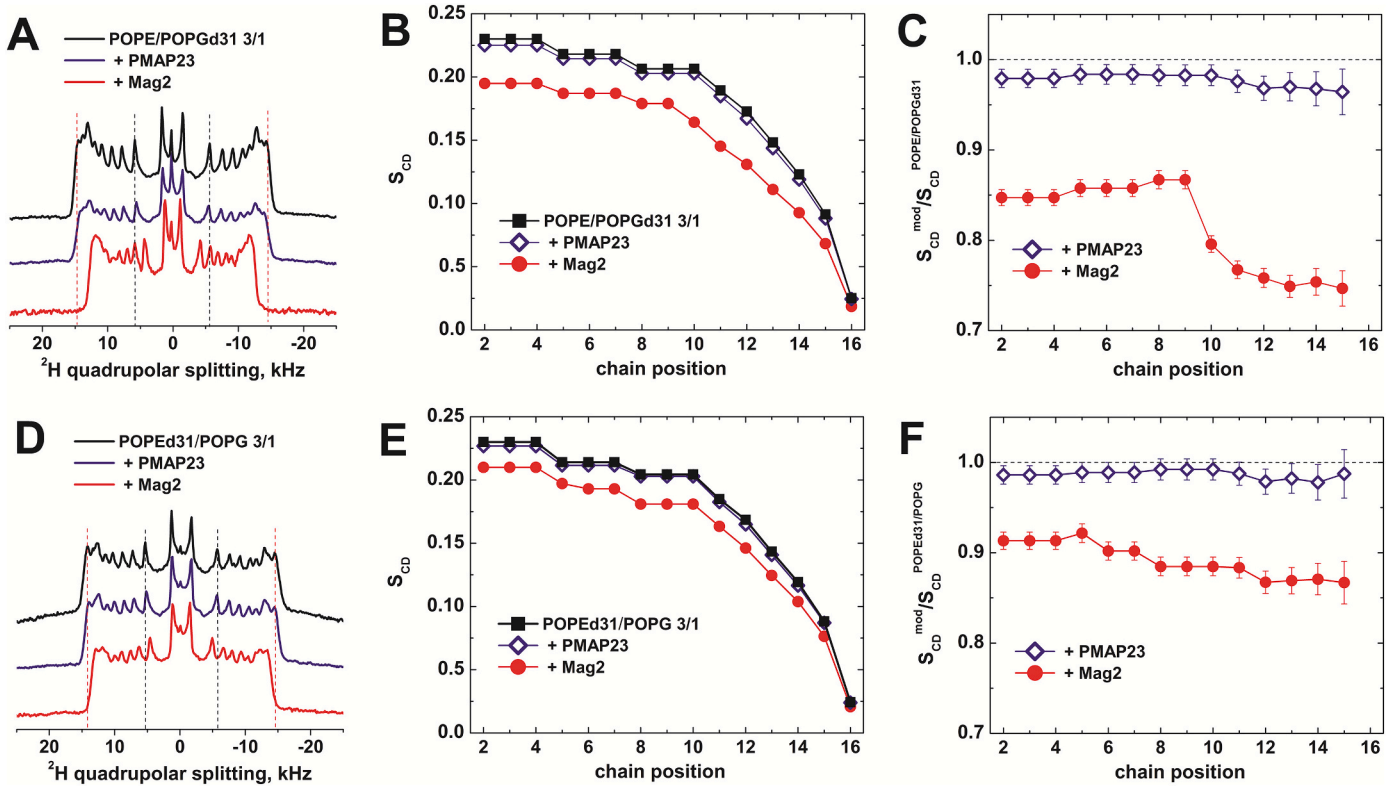

Fig. 12. Deuterium ssNMR spectra of POPE/POPG-d_{31} (3/1 molar ratio) (A-C) and POPE-d_{31}/POPG (3/1 molar ratio) membranes (D—F) in the absence and presence of PMAP-23 or magainin 2, both at a 2% mol/mol ratio with respect to the lipids. From the ^{2}H ssNMR spectra (A, D), the order parameters (B, E) and relative order parameters (C, F) were calculated for each segment. The temperature was set to 37 °C.

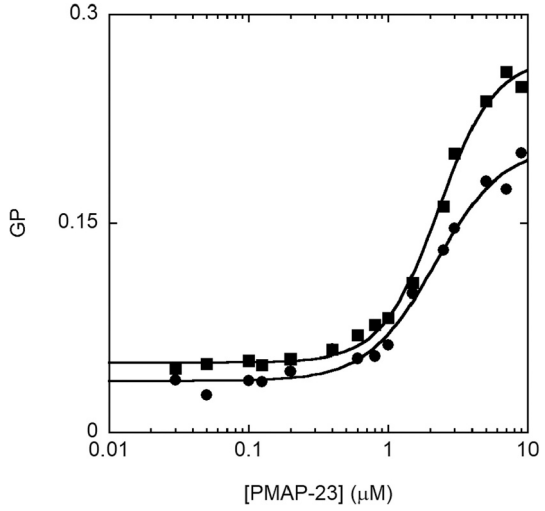

Fig. 13. Generalized polarization of laurdan inserted into POPC/POPG (2:1 molar ratio, squares) and POPE/POPG (3:1 molar ratio, circles) liposomes at increasing concentrations of PMAP-23. Lipid concentration 50 μM, laurdan to phospholipids molar ratio 1:100.

4. Discussion

The present systematic characterization by different fluorescence approaches of the effects of AMPs on the dynamics of the lipid bilayers showed that, irrespective of the mechanism of pore formation, they cause a global decrease in the mobility of liposomal membranes on the nanosecond time-scale, with a reduction in the rotational motions of probes positioned at different depths in the bilayer, in water penetration into the membrane and in the lateral diffusion of lipids. Similar effects were observed also in the membranes of *E. coli* bacteria. For the cationic AMP PMAP-23, these perturbations occurred in the same concentration range causing leakage in liposomes, and even started at concentrations lower than those causing bacterial killing, in *E. coli* cells. By contrast, for the hydrophobic, mainly transmembrane peptide alamethicin, pore formation took place already before the lipid dynamical changes appeared.

Sporadic observations of peptide-induced reductions in membrane fluidity, obtained with fluorescence or EPR spectroscopies appeared in the literature [80,3,91,92,93,94,95,96]. However, the simultaneous analysis of different aspects of membrane dynamics, reported here using peptides with different electrostatic properties, and acting according to distinct mechanisms, provides a comprehensive view of the phenomenon.

The findings presented here might indicate an additional mechanism of bactericidal activity, going beyond pore formation. As discussed in the introduction, correct fluidity of the membrane is essential for the life of bacteria. One of the reasons why membrane structure and dynamics are so crucial is that the function of membrane proteins is influenced by the physico-chemical properties of the bilayer, by directly regulating the function of membrane proteins, or their lateral distribution, diffusion, and interactions [23,97,98]. Therefore, the data presented here provide a solid experimental support to a hypothesis put forward several years ago: by perturbing the fluidity of the membrane, AMPs might act like "sand in a gearbox", and kill bacteria (also) by inhibiting the proper function of their membrane proteins [14].

Deuterium NMR studies of many cationic antimicrobial peptides that bind at the membrane interface have shown a reduction in lipid order [87,99,57,100], and a similar effect has been reproduced here for magainin 2. This has been explained by the intercalation of in-plane oriented helices into the membrane interface which causes the lipid fatty acyl chain to take over the extra volume within the hydrophobic

core of the membrane [56,49]. For the peptides on which the present study is focused (PMAP-23 and alamethicin), no significant decrease in order parameters has been observed.

The discrepancy between the lack of a perturbing effect observed in the ssNMR data presented here (or the lipid disordering observed for other peptides) and the reduced mobility and water penetration demonstrated by the fluorescence experiments is rather surprising. In principle, lipid order parameters should be directly correlated with the residual anisotropy of fluorescent probes or the generalized polarization of laurdan [101,102]. However, several sporadic results reported in the literature on the effects of AMPs on membrane dynamics are in agreement with the inconsistency between the two techniques observed in the present systematic study. A peptide-induced decrease in membrane fluidity has been repeatedly reported, based on fluorescence experiments. Just to provide some examples, an AMP-induced increase in laurdan GP has been reported for melittin [103], nisin [104], cWFW [95], thrombocidins-derived TC19 and TC84, and bactericidal peptide 2 [94]. Similarly, pHLIP [105], mesenterocin 52A [106], pep-1-K [80] and a cecropin A-melittin hybrid peptide [107] cause an increase in the anisotropy of DPH and DPH derivatives. By contrast, deuterium NMR studies of many cationic antimicrobial peptides that bind at the membrane interface have shown a reduction in lipid order [87,99,57,100]. While the present article was under review, a study was published, comparing the effects of membrane dynamics of the small molecule serotonin (rather than of a peptide), measured with different techniques [108]. A similar discrepancy between NMR and fluorescence (on a subset of the fluorophores and observables studied here) was reported.

An important difference between the two approaches is that fluorescence follows lipid motions indirectly, through the behavior of specific labels, while NMR measures the order and dynamics of acyl chain bonds directly. In principle, the variations in fluorescence properties could be just a direct effect of the peptide on the dynamics of adjacent fluorophores (e.g. by direct interaction, or by perturbing the probe position in the bilayer, moving it to a depth with different dynamic properties). However, we observed similar effects for different phenomena (water penetration, probe rotation, lipid translational diffusion) and for probes positioned at different depths. In the case of laurdan, binding of other peptides, even at high P/L ratios, has been demonstrated to not perturb the spectra [77]. In addition, even if the peptides were affecting nearby fluorescent labels directly, they would have a similar effect on surrounding lipids (and some of the probes used in the present study were covalently attached to lipids). Therefore, we can conclude that the observed perturbation of fluorophore dynamics corresponds to a real effect on membrane lipids and is not only an artifact limited to the probes.

Another main difference between fluorescence and NMR spectroscopies is that they report on very different timescales [59]. A reduced diffusional dynamics in the nanosecond times sampled by fluorescence could well coexist with an unperturbed lipid order or even with a higher disorder on the much longer NMR time frame. The crucial role of timescales in studies of membrane dynamics is supported by the observation of apparently contradictory results also for NMR and EPR, considering that the latter technique samples times in the ns, like fluorescence [59]. In the specific case of peptide effects on membrane dynamics, studied here, EPR has reported a reduction in membrane fluidity and an increase in lipid order [109,110,96]. For fluorescence and EPR, motions with correlation times longer than about 10 ns can be considered as “frozen”. By contrast, measurements of deuterium order parameters by NMR would not sense changes in correlation times which are much shorter than 10 μs [59]. Therefore, it is conceivable that the order parameter of individual C—D segments decrease even in situations where the membrane as an ensemble exhibits less freedom of motion.

While a reduction in NMR lipid order parameters has been often observed for cationic AMPs (and has been reproduced here for magainin 2), the two peptides investigated in the present study did not cause any significant effect. In the case of alamethicin, this behavior can be attributed to its hydrophobic character and to its predominant transmembrane orientation and is consistent with previous data [57]. In the case of the cationic PMAP-23, a possible interpretation for this peculiar behavior could be provided by the observation that the cationic charge of amphipathic AMPs that have been studied by ^{2}H ssNMR (and for which a membrane disordering effect has been reported) arises from the abundance of lysine residues [111,12,112,49]. By contrast, PMAP-23 is rich in arginines. Notably, Arg-rich peptides define a common class of cell penetrating peptides. When lipid bilayers in the presence Arg-rich cell penetrating peptides have been investigated by ^{2}H ssNMR spectroscopy, the pronounced disordering caused by Lys-rich AMPs is not as commonly observed and often absent [113,111,114,115]. SsNMR measurements provide evidence that, when compared to lysine, the guanidinium interactions with phosphates are more stable and involve hydrogen bonding [113,116,117]. However, the comparison of the effects on lipid order of Lys-rich AMPs, and Arg-rich CPPs might be complicated by the fact that the latter often adopt random coil and/or beta-sheet secondary structures at the membrane surface [113,117,118], while many AMPs (including PMAP-23 and magainin 2) are helical. Further studies will be required to verify the different properties of Lys and Arg rich peptides.

Regarding the possible mechanism of membrane stiffening by AMPs in the ns time-scale observed by fluorescence, it is worth mentioning that the effects reported here as a consequence of peptide addition resemble the electrostriction caused by divalent cations, such as Ca^{2+} [119,120], due to their strong electrostatic interaction with the phosphate groups of lipids. Considering the total positive net charge of PMAP-23 (+6), something similar could be taking place with this antimicrobial peptide. Indeed, clustering of negatively charged lipids around the peptide was implied by the FRET results, and it has been proposed that lipid domain formation could be one of the mechanisms of the bactericidal activity of AMPs [9,10]. However, by comparing data obtained at the same peptide concentration, the effects of alamethicin, which is neutral, were comparable to those of the cationic PMAP-23. Changes in fluorescence parameters occurred for both peptides above ~1 μM (at a 50 μM lipid concentration). Even considering possible differences in the fraction of membrane bound peptides under these conditions, this finding indicates that membrane dynamical changes are unspecific with regard to the peptide sequence and contradict a possible electrostatic origin of the peptide-induced stiffening. In addition, control experiments with vesicles completely formed by PG lipids showed peptide-induced effects on membrane dynamics comparable to those observed with PC/PG lipids (Supplemental Fig. 2). Since peptide-induced lateral separation of charged lipids cannot take place in membranes formed by PG lipids only, clustering of anionic lipids by the cationic PMAP-23, while present, can be ruled out as the main cause for the perturbation of bilayer dynamics.

Other effects, due to the steric hindrance caused by peptide association to the membrane might prevail. Even considering partial binding of the AMPs to the vesicle [27], the 1/50 peptide to lipid ratio at which dynamical effects start to be seen is rather high. In the case of PMAP-23, we demonstrated quantitatively that a very high membrane coverage is required for pore formation [29] and the present data show that for this peptide pore formation and perturbation of membrane dynamics take place at the same concentration, at least in vesicles. Due to their relative sizes, diffusion of peptide is considerably slower than that of the lipid [121,122] and one would expect that the peptides also hinder lipid diffusion when their concentration in the membrane is high enough.

Further studies are definitely needed to clarify the mechanism of peptide-induced reduction of lipid mobility in the ns time-scale. In any case, the present results expand the catalogue of peptide induced membrane perturbations and could lead to a better understanding of the bactericidal action of AMPs.

CRediT authorship contribution statement

Daniela Roversi: Methodology, Investigation, Data curation, Writing – review & editing, Visualization. **Cassandra Troiano:** Investigation, Data curation, Writing – review & editing, Visualization. **Evgeniy Salnikov:** Methodology, Investigation, Data curation, Writing – review & editing, Visualization. **Lorenzo Giordano:** Investigation, Visualization. **Francesco Riccitelli:** Investigation, Visualization. **Marta De Zotti:** Investigation, Resources, Funding acquisition. **Bruno Cascaro:** Investigation, Resources. **Maria Rosa Loffredo:** Investigation, Resources. **Yoonkyung Park:** Resources, Writing – review & editing. **Fernando Formaggio:** Methodology, Resources, Supervision, Project administration, Funding acquisition. **Maria Luisa Mangoni:** Methodology, Resources, Writing – review & editing, Supervision, Project administration. **Burkhard Bechinger:** Methodology, Writing – original draft, Supervision, Project administration, Funding acquisition. **Lorenzo Stella:** Conceptualization, Methodology, Writing – original draft, Visualization, Supervision, Project administration, Funding acquisition.

Declaration of Competing Interest

The authors declare that they have no known competing financial interests or personal relationships that could have appeared to influence the work reported in this paper.

Acknowledgements

This work was supported by the Italian Ministry for University and Research (MUR) (PRIN Project 2020833Y75 to LS and FF, and 20173LBZM2 to MDZ, and MUR-PNRR M4C2I1.3 PE6 project PE00000019 Heal Italia, to LS), AIRC IG2020 (24940 to LS), the Indo-French Centre for the Promotion of Advanced Research (IFCPAR/CEFIPRA; project no. 62T10-1, to BB), the Agence Nationale de la Recherche (projects Biosupramol 17-CE18-0033-3, Naturalarsenal 19-AMRB-0004-02, AmphiPep 20-CE18-0021, SAFEST 21-CE18-0043, AMLAA 21-CE11-0038-02 and the LabEx Chemistry of Complex Systems 10-LABX-0026_CSC, to BB), the University of Strasbourg (to BB), the CNRS (to BB), the Région Grand-Est (to BB), the Foundation Jean-Marie Lehn/International Center of Frontier Research in Chemistry (to BB) and the University of Padova (Project P-DiSC#04BIRD2019-UNIPD to MDZ and Uni-Impresa 2020-UNPD0Z9-0069266 to FF).

Appendix A. Supplementary data

Supplementary data to this article can be found online at https://doi.org/10.1016/j.bpc.2023.107060.

References

[1] S. Guha, J. Ghimire, E. Wu, W.C. Wimley, Mechanistic landscape of membrane-permeabilizing peptides, Chem. Rev. 119 (2019) 6040–6085.
[2] K. Matsuzaki (Ed.), Antimicrobial Peptides: Basics for Clinical Application, Springer, Singapore, 2019.
[3] G. Bocchinfuso, A. Palleschi, B. Orioni, G. Grande, F. Formaggio, C. Toniolo, Y. Park, K.-S. Hahm, L. Stella, Different mechanisms of action of antimicrobial peptides: insights from fluorescence spectroscopy experiments and molecular dynamics simulations, J. Pept. Sci. 15 (2009) 550–558.
[4] S. Das, K. Ben Haj Salah, E. Wenger, J. Martinez, J. Kotarba, V. Andreu, N. Ruiz, F. Savini, L. Stella, C. Didierjean, B. Legrand, N. Inguimbert, Enhancing the antimicrobial activity of alamethicin F50/5 by incorporating N-terminal hydrophobic triazole substituents, Chem. Eur. J. 23 (2017) 17964–17972.
[5] L. Stella, M. Burattini, C. Mazzuca, A. Palleschi, M. Venanzi, I. Coin, C. Peggion, C. Toniolo, B. Pispisa, Alamethicin interaction with lipid membranes: a spectroscopic study on synthetic analogues, Chem. Biodivers. 4 (2007) 1299–1312.
[6] R.F. Epand, M.A. Schmitt, S.H. Gellman, R.M. Epand, Role of membrane lipids in the mechanism of bacterial species selective toxicity by two α/β-antimicrobial peptides, Biochim. Biophys. Acta 1758 (2006) 1343–1350.
[7] R.F. Epand, B.P. Mowery, S.E. Lee, S.S. Stahl, R.I. Lehrer, S.H. Gellman, R. M. Epand, Dual mechanism of bacterial lethality for a cationic sequence-random copolymer that mimics host-defense antimicrobial peptides, J. Membr. Biol. 379 (2008) 38–50.
[8] R.M. Epand, S. Rotem, A. Mor, B. Berno, R.F. Epand, Bacterial membranes as predictors of antimicrobial potency, J. Am. Chem. Soc. 130 (2008) 14346–14352.
[9] R.M. Epand, R.F. Epand, Lipid domains in bacterial membranes and the action of antimicrobial agents, Biochim. Biophys. Acta 1788 (2009) 289–294.
[10] R.F. Epand, W.L. Maloy, A. Ramamoorthy, R.M. Epand, Probing the "Charge Cluster Mechanism" in amphipathic helical cationic antimicrobial peptides, Biochemistry. 49 (2010) 4076–4084.
[11] R.M. Epand, Anionic lipid clustering model, in: K. Matsuzaki (Ed.), Antimicrobial Peptides, Springer, Singapore, 2019, pp. 65–71.
[12] A.J. Mason, A. Martinez, C. Glaubitz, O. Danos, A. Kichler, B. Bechinger, The antibiotic and DNA-transfecting peptide LAH4 selectively associates with, and disorders, anionic lipids in mixed membranes, FASEB J. 20 (2006) 320–322.
[13] P. Wadhwani, R.F. Epand, N. Heidenreich, J. Bürck, A.S. Ulrich, R.M. Epand, Membrane-active peptides and the clustering of anionic lipids, Biophys. J. 103 (2012) 265–274.
[14] U. Pag, M. Oedenkoven, V. Sass, Y. Shai, O. Shamova, N. Antcheva, A. Tossi, H.-G. Sahl, Analysis of in vitro activities and modes of action of synthetic antimicrobial peptides derived from an α-helical 'sequence template', J. Antimicrob. Chemother. 61 (2008) 341–352.
[15] L. Beney, P. Gervais, Influence of the fluidity of the membrane on the response of microorganisms to environmental stresses, Appl. Microbiol. Biotechnol. 57 (2001) 34–42.
[16] T.J. Denich, L.A. Beaudette, H. Lee, J.T. Trevors, Effect of selected environmental and physico-chemical factors on bacterial cytoplasmic membranes, J. Microbiol. Methods 52 (2003) 149–182.
[17] D.A. Los, N. Murata, Membrane fluidity and its roles in the perception of environmental signals, Biochim. Biophys. Acta 1666 (2004) 142–157.
[18] S. Morein, A.-S. Andersson, L. Rilfors, G. Lindblom, Wild-type *Escherichia coli* cells regulate the membrane lipid composition in a "window" between gel and non-lamellar structures, J. Biol. Chem. 271 (1996) 6801–6809.
[19] P.J. Quinn, The fluidity of cell membranes and its regulation, Prog. Biophys. Mol. Biol. 38 (1981) 1–104.
[20] N. Russell, Mechanisms of thermal adaptation in bacteria: blueprints for survival, Trends Biochem. Sci. 9 (1984) 108–112.
[21] M. Sinensky, Homeoviscous adaptation—a homeostatic process that regulates the viscosity of membrane lipids in *Escherichia coli*, Proc. Natl. Acad. Sci. U. S. A. 71 (1974) 522–525.
[22] Y.-M. Zhang, C.O. Rock, Membrane lipid homeostasis in bacteria, Nat. Rev. Microbiol. 6 (2008) 222–233.
[23] M. Gohrbandt, A. Lipski, J.W. Grimshaw, J.A. Buttress, Z. Baig, B. Herkenhoff, S. Walter, R. Kurre, G. Deckers-Hebestreit, H. Strahl, Low membrane fluidity triggers lipid phase separation and protein segregation in living bacteria, EMBO J. 41 (2022), e109800.
[24] J.H. Kang, S.Y. Shin, S.Y. Jang, K.L. Kim, K.-S. Hahm, Effects of tryptophan residues of porcine myeloid antibacterial peptide PMAP-23 on antibiotic activity, Biochem. Biophys. Res.Comm. 264 (1999) 281–286.
[25] D.G. Lee, D.-H. Kim, Y. Park, H.K. Kim, H.N. Kim, Y.K. Shin, C.H. Choi, K.-S. Hahm, Fungicidal effect of antimicrobial peptide, PMAP-23, isolated from porcine myeloid against *Candida albicans*, Biochem. Biophys. Res.Comm. 282 (2001) 570–574.
[26] M. Zanetti, P. Storici, A. Tossi, M. Scocchi, R. Gennaro, Molecular cloning and chemical synthesis of a novel antibacterial peptide derived from pig myeloid cells, J. Biol. Chem. 269 (1994) 7855–7858.
[27] B. Orioni, G. Bocchinfuso, J.Y. Kim, A. Palleschi, G. Grande, S. Bobone, Y. Park, J. I. Kim, K. Hahm, L. Stella, Membrane perturbation by the antimicrobial peptide PMAP-23: a fluorescence and molecular dynamics study, Biochim. Biophys. Acta 1788 (2009) 1523–1533.
[28] K. Park, D. Oh, S. Yub Shin, K.-S. Hahm, Y. Kim, Structural studies of porcine myeloid antibacterial peptide PMAP-23 and its analogues in DPC micelles by NMR spectroscopy, Biochem. Biophys. Res. Commun. 290 (2002) 204–212.
[29] D. Roversi, V. Luca, S. Aureli, Y. Park, M.L. Mangoni, L. Stella, How many antimicrobial peptide molecules kill a bacterium? The case of PMAP-23, ACS Chem. Biol. 9 (2014) 2003–2007.
[30] F. Savini, V. Luca, A. Bocedi, R. Massoud, Y. Park, M.L. Mangoni, L. Stella, Cell-density dependence of host-defense peptide activity and selectivity in the presence of host cells, ACS Chem. Biol. 12 (2017) 52–56.
[31] F. Savini, M.R. Loffredo, C. Troiano, S. Bobone, N. Malanovic, T.O. Eichmann, L. Caprio, V.C. Canale, Y. Park, M.L. Mangoni, L. Stella, Binding of an antimicrobial peptide to bacterial cells: interaction with different species, strains and cellular components, Biochim. Biophys. Acta 1862 (2020), 183291.
[32] B. Leitgeb, A. Szekeres, L. Manczinger, C. Vágvölgyi, L. Kredics, The history of Alamethicin: a review of the Most extensively studied peptaibol, Chem. Biodivers. 4 (2007) 1027–1051.
[33] R.O. Fox, F.M. Richards, A voltage-gated ion channel model inferred from the crystal structure of alamethicin at 1.5-Å resolution, Nature 300 (1982) 325–330.
[34] R. Improta, N. Rega, C. Aleman, V. Barone, Conformational behavior of macromolecules in solution, homopolypeptides of α-aminoisobutyric acid as test cases, Macromolecules 34 (2001) 7550–7557.
[35] W.-C. Jen, G.A. Jones, D. Brewer, V.O. Parkinson, A. Taylor, The antibacterial activity of alamethicins and zervamicins, J. Appl. Bacteriol. 63 (1987) 293–298.
[36] C.E. Meyer, F. Reusser, A polypeptide antibacterial agent isolated fromTrichoderma viride, Experientia. 23 (1967) 85–86.

[37] H. Duclohier, H. Wróblewski, Voltage-dependent pore formation and antimicrobial activity by alamethicin and analogues, J. Membr. Biol. 184 (2001) 1–12.

[38] K. He, S.J. Ludtke, H.W. Huang, D.L. Worcester, Antimicrobial peptide pores in membranes detected by neutron in-plane scattering, Biochemistry. 34 (1995) 15614–15618.

[39] S. Qian, W. Wang, L. Yang, H.W. Huang, Structure of transmembrane pore induced by Bax-derived peptide: evidence for lipidic pores, Proc. Natl. Acad. Sci. U. S. A. 105 (2008) 17379–17383.

[40] B. Bechinger, Structure and functions of channel-forming peptides: magainins, cecropins, melittin and alamethicin, J. Membr. Biol. 156 (1997) 197–211.

[41] D. Noshiro, K. Asami, S. Futaki, Metal-assisted channel stabilization: disposition of a single histidine on the N-terminus of alamethicin yields channels with extraordinarily long lifetimes, Biophys. J. 98 (2010) 1801–1808.

[42] E.S. Salnikov, J. Raya, M. De Zotti, E. Zaitseva, C. Peggion, G. Ballano, C. Toniolo, J. Raap, B. Bechinger, Alamethicin supramolecular organization in lipid membranes from ^{19}F solid-state NMR, Biophys. J. 111 (2016) 2450–2459.

[43] M.S.P. Sansom, Alamethicin and related peptaibols – Model ion channels, Eur. Biophys. J. 22 (1993).

[44] M.S.P. Sansom, Structure and function of channel-forming peptaibols, Q. Rev. Biophys. 26 (1993) 365–421.

[45] M. Bak, R.P. Bywater, M. Hohwy, J.K. Thomsen, K. Adelhorst, H.J. Jakobsen, O. W. Sørensen, N.C. Nielsen, Conformation of Alamethicin in oriented phospholipid bilayers determined by ^{15} N solid-state nuclear magnetic resonance, Biophys. J. 81 (2001) 1684–1698.

[46] B. Bechinger, D.A. Skladnev, A. Ogrel, X. Li, E.V. Rogozhkina, T.V. Ovchinnikova, J.D.J. O'Neil, J. Raap, ^{15} N and ^{31} P solid-state NMR investigations on the orientation of zervamicin II and alamethicin in phosphatidylcholine membranes, Biochemistry. 40 (2001) 9428–9437.

[47] C.L. North, M. Barranger-Mathys, D.S. Cafiso, Membrane orientation of the N-terminal segment of alamethicin determined by solid-state ^{15} N NMR, Biophys. J. 69 (1995) 2392–2397.

[48] E.S. Salnikov, H. Friedrich, X. Li, P. Bertani, S. Reissmann, C. Hertweck, J.D. J. O'Neil, J. Raap, B. Bechinger, Structure and alignment of the membrane-associated peptaibols ampullosporin a and alamethicin by oriented ^{15}N and ^{31}P solid-state NMR spectroscopy, Biophys. J. 96 (2009) 86–100.

[49] E. Salnikov, C. Aisenbrey, V. Vidovic, B. Bechinger, Solid-state NMR approaches to measure topological equilibria and dynamics of membrane polypeptides, Biochim. Biophys. Acta 1798 (2010) 258–265.

[50] B. Bechinger, Towards membrane protein design: pH-sensitive topology of histidine-containing polypeptides, J. Mol. Biol. 263 (1996) 768–775.

[51] E. Salnikov, C. Aisenbrey, B. Bechinger, Lipid saturation and head group composition have a pronounced influence on the membrane insertion equilibrium of amphipathic helical polypeptides, Biochim. Biophys. Acta 1864 (2022), 183844.

[52] G. Bocchinfuso, S. Bobone, C. Mazzuca, A. Palleschi, L. Stella, Fluorescence spectroscopy and molecular dynamics simulations in studies on the mechanism of membrane destabilization by antimicrobial peptides, Cell. Mol. Life Sci. 68 (2011) 2281–2301.

[53] F.S. Abrams, E. London, Extension of the parallax analysis of membrane penetration depth to the polar region of model membranes: use of fluorescence quenching by a spin-label attached to the phospholipid polar headgroup, Biochemistry. 32 (1993) 10826–10831.

[54] C.C. De Vequi-Suplicy, C.R. Benatti, M.T. Lamy, Laurdan in fluid bilayers: position and structural sensitivity, J. Fluoresc. 16 (2006) 431–439.

[55] R.D. Kaiser, E. London, Location of diphenylhexatriene (DPH) and its derivatives within membranes: comparison of different fluorescence quenching analyses of membrane depth, Biochemistry. 37 (1998) 8180–8190.

[56] C. Aisenbrey, A. Marquette, B. Bechinger, The mechanisms of action of cationic antimicrobial peptides refined by novel concepts from biophysical investigations, in: K. Matsuzaki (Ed.), Antimicrobial Peptides, Springer, Singapore, 2019, pp. 33–64.

[57] E.S. Salnikov, A.J. Mason, B. Bechinger, Membrane order perturbation in the presence of antimicrobial peptides by 2H solid-state NMR spectroscopy, Biochimie. 91 (2009) 734–743.

[58] S.L. Veatch, I.V. Polozov, K. Gawrisch, S.L. Keller, Liquid domains in vesicles investigated by NMR and fluorescence microscopy, Biophys. J. 86 (2004) 2910–2922.

[59] K. Gawrisch, The dynamics of membrane lipids, in: P.L. Yeagle (Ed.), The Structure of Biological Membranes, 2nd ed., CRC Press, 2004.

[60] C. Peggion, I. Coin, C. Toniolo, Total synthesis in solution of alamethicin F50/5 by an easily tunable segment condensation approach, Pept. Sci. 76 (2004) 485–493.

[61] C. Mazzuca, B. Orioni, M. Coletta, F. Formaggio, C. Toniolo, G. Maulucci, M. De Spirito, B. Pispisa, M. Venanzi, L. Stella, Fluctuations and the rate-limiting step of peptide-induced membrane leakage, Biophys. J. 99 (2010) 1791–1800.

[62] J.C.M. Stewart, Colorimetric determination of phospholipids with ammonium ferrothiocyanate, Anal. Biochem. 104 (1980) 10–14.

[63] J.H. Davis, K.R. Jeffrey, M. Bloom, M.I. Valic, T.P. Higgs, Quadrupolar echo deuteron magnetic resonance spectroscopy in ordered hydrocarbon chains, Chem. Phys. Lett. 42 (1976) 390–394.

[64] L.S. Batchelder, C.H. Niu, D.A. Torchia, Methyl reorientation in polycrystalline amino acids and peptides: a deuteron NMR spin-lattice relaxation study, J. Am. Chem. Soc. 105 (1983) 2228–2231.

[65] S. Bobone, L. Stella, L., Selectivity of antimicrobial peptides: A complex interplay of multiple equilibria, in: K. Matsuzaki (Ed.), Antimicrobial Peptides: Basics for Clinical Application, Springer, 2019, pp. 175–214.

[66] S. Mukherjee, H. Raghuraman, S. Dasgupta, A. Chattopadhyay, Organization and dynamics of N-(7-nitrobenz-2-oxa-1, 3-diazol-4-yl)-labeled lipids: a fluorescence approach, Chem. Phys. Lipids 127 (2004) 91–101.

[67] D.E. Wolf, A.P. Winiski, A.E. Ting, K.M. Bocian, R.E. Pagano, Determination of the transbilayer distribution of fluorescent lipid analogs by nonradiative fluorescence resonance energy transfer, Biochemistry 31 (1992) 2865–2873.

[68] A. Kyrychenko, M.V. Rodnin, A.S. Ladokhin, Calibration of distribution analysis of the depth of membrane penetration using simulations and depth-dependent fluorescence quenching, J. Membr. Biol. 248 (2015) 583–594.

[69] H.A. Filipe, L.S. Santos, J.P. Ramalho, M.J. Moreno, L.M. Loura, Behaviour of NBD-head group labelled phosphatidylethanolamines in POPC bilayers: a molecular dynamics study, Phys. Chem. Chem. Phys. 17 (2015) 20066–20079.

[70] A.M. do Canto, J.R. Robalo, P.D. Santos, A.J.P. Carvalho, J.P. Ramalho, L. M. Loura, Diphenylhexatriene membrane probes DPH and TMA-DPH: a comparative molecular dynamics simulation study, Biochim. Biophys. Acta 1858 (2016) 2647–2661.

[71] I. Hurjui, A. Neamtu, D.O. Dorohoi, The interaction of fluorescent DPH probes with unsaturated phospholipid membranes: a molecular dynamics study, J. Mol. Struct. 1044 (2013) 134–139.

[72] M. Paloncýová, M. Ameloot, M.S. Knippenberg, Orientational distribution of DPH in lipid membranes: a comparison of molecular dynamics calculations and experimental time-resolved anisotropy experiments, Phys. Chem. Chem. Phys. 21 (2019) 7594–7604.

[73] E. Pebay-Peyroula, E.J. Dufourc, A.G. Szabo, Location of diphenyl-hexatriene and trimethylammonium-diphenyl-hexatriene in dipalmitoylphosphatidylcholine bilayers by neutron diffraction, Biophys. Chem. 53 (1994) 45–56.

[74] S.S. Antollini, F.J. Barrantes, Disclosure of discrete sites for phospholipid and sterols at the protein– lipid interface in native acetylcholine receptor-rich membrane, Biochemistry 37 (1998) 16653–16662.

[75] P. Jurkiewicz, A. Olżyńska, M. Langner, M. Hof, Headgroup hydration and mobility of DOTAP/DOPC bilayers: a fluorescence solvent relaxation study, Langmuir 22 (2006) 8741–8749.

[76] J. Barucha-Kraszewska, S. Kraszewski, C. Ramseyer, Will C-Laurdan dethrone Laurdan in fluorescent solvent relaxation techniques for lipid membrane studies? Langmuir 29 (2013) 1174–1182.

[77] J. Dinic, H. Biverståhl, L. Mäler, I. Parmryd, Laurdan and di-4-ANEPPDHQ do not respond to membrane-inserted peptides and are good probes for lipid packing, Biochim. Biophys. Acta 1808 (2011) 298–306.

[78] E.K. Krasnowska, E. Gratton, T. Parasassi, Prodan as a membrane surface fluorescence probe: partitioning between water and phospholipid phases, Biophys. J. 74 (1998) 1984–1993.

[79] J. Martins, E. Melo, Molecular mechanism of lateral diffusion of py10-PC and free pyrene in fluid DMPC bilayers, Biophys. J. 80 (2001) 832–840.

[80] S. Bobone, A. Piazzon, B. Orioni, J.Z. Pedersen, Y.H. Nan, K.-S. Hahm, S.Y. Shin, L. Stella, The thin line between cell-penetrating and antimicrobial peptides: the case of Pep-1 and Pep-1-K, J. Pept. Sci. 17 (2011) 335–341.

[81] A. Marquette, B. Lorber, B. Bechinger, Reversible liposome association induced by LAH4: a peptide with potent antimicrobial and nucleic acid transfection activities, Biophys. J. 98 (11) (2010) 2544–2553.

[82] L.J. Bessa, M. Ferreira, P. Gameiro, Evaluation of membrane fluidity of multidrug-resistant isolates of *Escherichia coli* and *Staphylococcus aureus* in presence and absence of antibiotics, J. Photochem. Photobiol. B 181 (2018) 150–156.

[83] S. Mazor, T. Regev, E. Mileykovskaya, W. Margolin, W. Dowhan, I. Fishov, Mutual effects of MinD–membrane interaction: I. changes in the membrane properties induced by MinD binding, Biochim. Biophys. Acta 1778 (2008) 2496–2504.

[84] N.C.S. Mykytczuk, J.T. Trevors, L.G. Leduc, G.D. Ferroni, Fluorescence polarization in studies of bacterial cytoplasmic membrane fluidity under environmental stress, Prog. Biophys. Mol. Biol. 95 (2007) 60–82.

[85] S.A. Mohid, P. Sharma, A. Alghalayini, T. Saini, D. Datta, M.D. Willcox, H. Ali, S. Raha, A. Singha, D.K. Lee, N. Sahoo, C.G. Cranfield, S. Roy, A. Bhunia, A rationally designed synthetic antimicrobial peptide against Pseudomonas-associated corneal keratitis: structure-function correlation, Biophys. Chem. 286 (2022), 106802.

[86] T. Won, S.A. Mohid, J. Choi, M. Kim, J. Krishnamoorthy, I. Biswas, A. Bhunia, D. K. Lee, The role of hydrophobic patches of de novo designed MSI-78 and VG16KRKP antimicrobial peptides on fragmenting model bilayer membranes, Biophys. Chem. 296 (2023), 106981.

[87] N. Harmouche, B. Bechinger, Lipid-mediated interactions between the antimicrobial peptides magainin 2 and PGLa in bilayers, Biophys. J. 115 (2018) 1033–1044.

[88] B. Bechinger, The structure, dynamics and orientation of antimicrobial peptides in membranes by multidimensional solid-state NMR spectroscopy, Biochim. Biophys. Acta 1462 (1999) 157–183.

[89] B. Bechinger, Detergent-like properties of magainin antibiotic peptides: a 31P solid-state NMR spectroscopy study, Biochim. Biophys. Acta 1712 (2005) 101–108.

[90] K. Matsuzaki, O. Murase, H. Tokuda, S. Funakoshi, N. Fujii, K. Miyajima, Orientational and aggregational states of magainin 2 in phospholipid bilayers, Biochemistry. 33 (1994) 3342–3349.

[91] T. Kikukawa, T. Araiso, Changes in lipid mobility associated with alamethicin incorporation into membranes, Arch. Biochem. Biophys. 405 (2002) 214–222.

[92] S. Ladha, A.R. Mackie, L.J. Harvey, D.C. Clark, E.J. Lea, M. Brullemans, H. Duclohier, Lateral diffusion in planar lipid bilayers: a fluorescence recovery

after photobleaching investigation of its modulation by lipid composition, cholesterol, or alamethicin content and divalent cations, Biophys. J. 71 (1996) 1364–1373.
[93] A.L. Lai, J.H. Freed, HIV gp41 fusion peptide increases membrane ordering in a cholesterol-dependent fashion, Biophys. J. 106 (2014) 172–181.
[94] S. Omardien, J.W. Drijfhout, F.M. Vaz, M. Wenzel, L.W. Hamoen, S.A.J. Zaat, S. Brul, Bactericidal activity of amphipathic cationic antimicrobial peptides involves altering the membrane fluidity when interacting with the phospholipid bilayer, Biochim. Biophys. Acta 1860 (2018) 2404–2415.
[95] K. Scheinpflug, M. Wenzel, O. Krylova, J.E. Bandow, M. Dathe, H. Strahl, Antimicrobial peptide cWFW kills by combining lipid phase separation with autolysis, Sci. Rep. 7 (2017) 44332.
[96] C. Watala, K. Gwoździński, Melittin-induced alterations in dynamic properties of human red blood cell membranes, Chem. Biol. Interact. 82 (1992) 135–149.
[97] I. Levental, E. Lyman, Regulation of membrane protein structure and function by their lipid nano-environment, Nat. Rev. Mol. Cell Biol. 24 (2023) 79.
[98] K. Yoshida, S. Nagatoishi, D. Kuroda, N. Suzuki, T. Murata, K. Tsumoto, Phospholipid membrane fluidity alters ligand binding activity of a G protein-coupled receptor by shifting the conformational equilibrium, Biochemistry. 58 (2019) 504–508.
[99] J. Pius, M.R. Morrow, V. Booth, ^{2}H solid-state nuclear magnetic resonance investigation of whole *Escherichia coli* interacting with antimicrobial peptide MSI-78, Biochemistry. 51 (2012) 118–125.
[100] N.P. Santisteban, M.R. Morrow, V. Booth, Effect of AMPs MSI-78 and BP100 on the lipid acyl chains of 2H-labeled intact gram positive bacteria, Biochim. Biophys. Acta 1862 (2020), 183199.
[101] A. Kintanar, A.C. Kunwar, E. Oldfield, Deuterium nuclear magnetic resonance spectroscopic study of the fluorescent probe diphenylhexatriene in model membrane systems, Biochemistry. 25 (1986) 6517–6524.
[102] S.S.W. Leung, J. Brewer, L.A. Bagatolli, J.L. Thewalt, Measuring molecular order for lipid membrane phase studies: linear relationship between Laurdan generalized polarization and deuterium NMR order parameter, Biochim. Biophys. Acta 1861 (2019), 183053.
[103] B. Zorilă, G. Necula, M. Radu, M. Bacalum, Melittin induces local order changes in artificial and biological membranes as revealed by spectral analysis of Laurdan fluorescence, Toxins. 12 (2020) 705.
[104] S.B. Nielsen, D.E. Otzen, Impact of the antimicrobial peptide Novicidin on membrane structure and integrity, J. Colloid Interface Sci. 345 (2010) 248–256.
[105] M. Zoonens, Y.K. Reshetnyak, D.M. Engelman, Bilayer interactions of pHLIP, a peptide that can deliver drugs and target tumors, Biophys. J. 95 (2008) 225–235.
[106] J. Jasniewski, C. Cailliez-Grimal, M. Younsi, J.B. Millière, A.M. Revol-Junelles, Fluorescence anisotropy analysis of the mechanism of action of mesenterocin 52A: speculations on antimicrobial mechanism, Appl. Microbiol. Biotechnol. 81 (2008) 339–347.
[107] J.M. Mancheño, M. Oñaderra, A. Martínez del Pozo, P. Díaz-Achirica, D. Andreu, L. Rivas, J.G. Gavilanes, Release of lipid vesicle contents by an antibacterial cecropin a – melittin hybrid peptide, Biochemistry 35 (1996) 9892–9899.
[108] A. Gupta, M. Kallianpur, D.S. Roy, O. Engberg, H. Chakrabarty, D. Huster, S. Maiti, Different membrane order measurement techniques are not mutually consistent, Biophys. J. 122 (2023) 964–972.
[109] M. Ge, J.H. Freed, Fusion peptide from influenza hemagglutinin increases membrane surface order: an electron-spin resonance study, Biophys. J. 96 (2009) 4925–4934.
[110] M. Ge, J.H. Freed, Two conserved residues are important for inducing highly ordered membrane domains by the transmembrane domain of influenza hemagglutinin, Biophys. J. 100 (2011) 90–97.
[111] B. Kwon, A.J. Waring, M. Hong, A ^{2}H solid-state NMR study of lipid clustering by cationic antimicrobial and cell-penetrating peptides in model bacterial membranes, Biophys. J. 105 (2013) 2333–2342.
[112] A. Ramamoorthy, S. Thennarasu, D.-K. Lee, A. Tan, L. Maloy, Solid-state NMR investigation of the membrane-disrupting mechanism of antimicrobial peptides MSI-78 and MSI-594 derived from magainin 2 and melittin, Biophys. J. 91 (2006) 206–216.
[113] F. Jean-François, S. Castano, B. Desbat, B. Odaert, M. Roux, M.-H. Metz-Boutigue, E.J. Dufourc, Aggregation of Cateslytin β-sheets on negatively charged lipids promotes rigid membrane domains. A new mode of action for antimicrobial peptides? Biochemistry. 47 (2008) 6394–6402.
[114] A. Lamazière, O. Maniti, C. Wolf, O. Lambert, G. Chassaing, G. Trugnan, J. Ayala-Sanmartin, Lipid domain separation, bilayer thickening and pearling induced by the cell penetrating peptide penetratin, Biochim. Biophys. Acta 1798 (2010) 2223–2230.
[115] K. Witte, B.E.S. Olausson, A. Walrant, I.D. Alves, A. Vogel, Structure and dynamics of the two amphipathic arginine-rich peptides RW9 and RL9 in a lipid environment investigated by solid-state NMR and MD simulations, Biochim. Biophys. Acta 1828 (2013) 824–833.
[116] Y. Su, T. Doherty, A.J. Waring, P. Ruchala, M. Hong, Roles of arginine and lysine residues in the translocation of a cell-penetrating peptide from ^{13}C, ^{31}P, and ^{19}F solid-state NMR, Biochemistry. 48 (2009) 4587–4595.
[117] Y. Su, A.J. Waring, P. Ruchala, M. Hong, Membrane-bound dynamic structure of an arginine-rich cell-penetrating peptide, the protein transduction domain of HIV TAT, from solid-state NMR, Biochemistry. 49 (2010) 6009–6020.
[118] M. Sugawara, J.M. Resende, C.M. Moraes, A. Marquette, J. Chich, M. Metz-Boutigue, B. Bechinger, Membrane structure and interactions of human catestatin by multidimensional solution and solid-state NMR spectroscopy, FASEB J. 24 (2010) 1737–1746.
[119] O. Szekely, A. Steiner, P. Szekely, E. Amit, R. Asor, C. Tamburu, U. Raviv, The structure of ions and zwitterionic lipids regulates the charge of dipolar membranes, Langmuir. 27 (2011) 7419–7438.
[120] R.S. Vest, L.J. Gonzales, S.A. Permann, E. Spencer, L.D. Hansen, A.M. Judd, J. D. Bell, Divalent cations increase lipid order in erythrocytes and susceptibility to secretory phospholipase A2, Biophys. J. 86 (2004) 2251–2260.
[121] C. Aisenbrey, B. Bechinger, Investigations of polypeptide rotational diffusion in aligned membranes by ^{2}H and ^{15}N solid-state NMR spectroscopy, J. Am. Chem. Soc. 126 (2004) 16676–16683.
[122] J.M. Sanderson, Resolving the kinetics of lipid, protein and peptide diffusion in membranes, Mol. Membr. Biol. 29 (2012) 118–143.